Improved P-f/Q-V and P-V/Q-f Droop Controllers for Parallel Distributed Generation Inverters in AC Microgrid

Article *in* Sustainable Cities and Society · May 2018

DOI: 10.1016/j.scs.2018.04.026

3 authors, including:

Josep M. Guerrero
Aalborg University
842 PUBLICATIONS **21,628** CITATIONS

SEE PROFILE

Improved *P-f/Q-V* and *P-V/Q-f* Droop Controllers for Parallel Distributed Generation Inverters in AC Microgrid

Chethan Raj D[a,*], D.N. Gaonkara, Josep M. Guerrero[b]

[a]Department of Electrical and Electronics Engineering, NITK, Surathkal, Mangalore, India
[b]Department of Energy Technology, Aalborg University, Aalborg, Denmark joz@et.aau.dk

Abstract-Distributed generation inverters are generally operated in parallel with *P-f/Q-V* and *P-V/Q-f* droop control strategies. Due to mismatched resistive and inductive line impedance, power sharing and output voltage of the parallel DG inverters deviate from the reference value. This leads to instability in the microgrid system. Adding virtual resistors and virtual inductors in the control loop of droop controllers improve the power sharing and stability of operation. But, this leads to voltage drop. Therefore, an improved *P-f/Q-V* and *P-V/Q-f* droop control is proposed. Simulation results demonstrate that the proposed control and the selection of parameters enhance the output voltage of inverters.

Keywords-Distributed generation inverters, droop control, microgrid, output impedance, virtual resistors, virtual inductors.

1. Introduction

Distributed generation (DG) systems use renewable energy resources such as wind, solar, tidal energy, and some non-renewable energy sources such as fuel cells, gas turbines, micro-turbines, and generators [1]. As compared to traditional power systems, DG systems are decentralized and highly flexible [2]. Hence, accounts for reduced transmission cost and improved stability and reliability of power systems [2]. The distributed power supply in DG systems is not controllable. When directly connected, causes negative impact on the power grid [3]. To avoid this adverse effect on the power grid, United States Electrical Reliability Technology Solutions Consortium has studied the role of distributed power in low-voltage power grids and proposed the concept microgrid [4],[5].

Microgrid can be categorized as AC, DC and AC-DC microgrids [5], [6],[7]. In AC microgrids the parallel operation of DG inverters can be divided into wired and wireless parallel control. Wired parallel control include circular chain control (3C) [8], centralized control [9], and master slave control [10], among others. Wired parallel control strategy uses interconnected signal lines for communication between the DG inverters. However, too many communication signal lines leads to a complex structure of the microgrid and inhibits expansion. In order to solve the signal line problem of wired interconnection control, a wireless parallel control strategy

based on active and reactive power droop control is proposed [11], [12]. Wireless control includes droop control [10], [12],[33] reverse droop control [14], hierarchical droop control [12], improved droop control [15], [16], [17] and virtual power droop control [18], among others.

Droop control in a microgrid has a broad application prospects, as it does not require physical communication links and easy to achieve plug and play operation [11]. The traditional *P-f/Q-V* droop control and *P-V/Q-f* droop control as the research background, the main research is summarized on the following aspects: Droop decoupling control strategy [12], droop coefficient self-tuning optimization algorithm [19], virtual impedance control [20], [21]. In an inductive line environment, droop control can achieve better results. But, mostly for microgrid voltage level of 10 kV the line impedance is resistive, thus affects the droop control performance. The use of traditional droop control method makes it difficult to achieve precise power sharing and circulation suppression [22]. A variety of improved droop control methods are proposed. In [23], [24] an improved droop control is proposed by designing control parameters, so that the inverter output impedance is always inductive. However, this method has a limited range of effective output impedance adjustment. In [25], by adding differential links in the traditional droop control equation, the power sharing of the parallel DG inverter is quickly stabilized. But this leads to harmonic amplification and output voltage distortion. Virtual impedance method [20], [21], [26] is adopted for parallel DG inverters to improve power sharing under different line conditions. However, virtual impedance does not completely eliminate the influence of line impedance and increases the voltage drop. In an actual microgrid system, differences in parameters and line impedance, makes active and reactive powers not completely decoupled, thus affecting the accuracy of the droop controllers.

In view of the aforesaid problem, by amplitude frequency characteristics analysis, different control parameters effects on the output impedance of DG inverters and appropriate control parameters are selected. In order to solve the parameters differences and uneven distribution of power between the parallel DG inverters in a microgrid, virtual resistors and inductors are added into the control loop of the droop controllers. The introduction of virtual resistors and inductors cause DG inverter output voltage to drop. In order to reinstate the effect, an improved *P-f/Q-V* and *P-V/Q-f* droop with secondary control is proposed.

The paper is organized as follows. In Section 2, power flow characteristics of droop control is presented for DG inverters. In Section 3, dual loop control parameters are altered using virtual resistors and inductors for improving power sharing between DG inverters and also secondary control is proposed to improve the voltage deviations. In Section 4, simulation results are presented. Finally, the concluding remarks are deliberated in Section 5.

2. Droop control basic principle

2.1 Power flow characteristics between equivalent voltage sources

A simplified schematic of parallel DG inverters is shown in Fig.1. The sum of the output impedance of the inverter and the line impedance of DG inverter1 and DG inverter2 is given by

$$Z_1 = r_1 + jx_1 + R_{1Line} + jX_{1Line} = Z_1\angle\theta_1,$$

$$Z_2 = r_2 + jx_2 + R_{2Line} + jX_{2Line} = Z_2\angle\theta_2 .$$

where r_1, r_2 are the DG inverters equivalent output resistances; x_1, x_2 are the inverter equivalent output reactances; R_{1Line}, R_{2Line} are the line resistances; X_{1Line}, X_{2Line} are the line reactances; $V_{com}\angle 0$ is the ac bus voltage amplitude; V_1, V_2 are DG inverter output voltages; δ_1, δ_2 are the DG inverter output voltage phase angles; θ_1, θ_2 are the total impedance angles of DG inverters; i_{o1}, i_{o2} are the output currents of DG inverters; i_o is the load current [27].

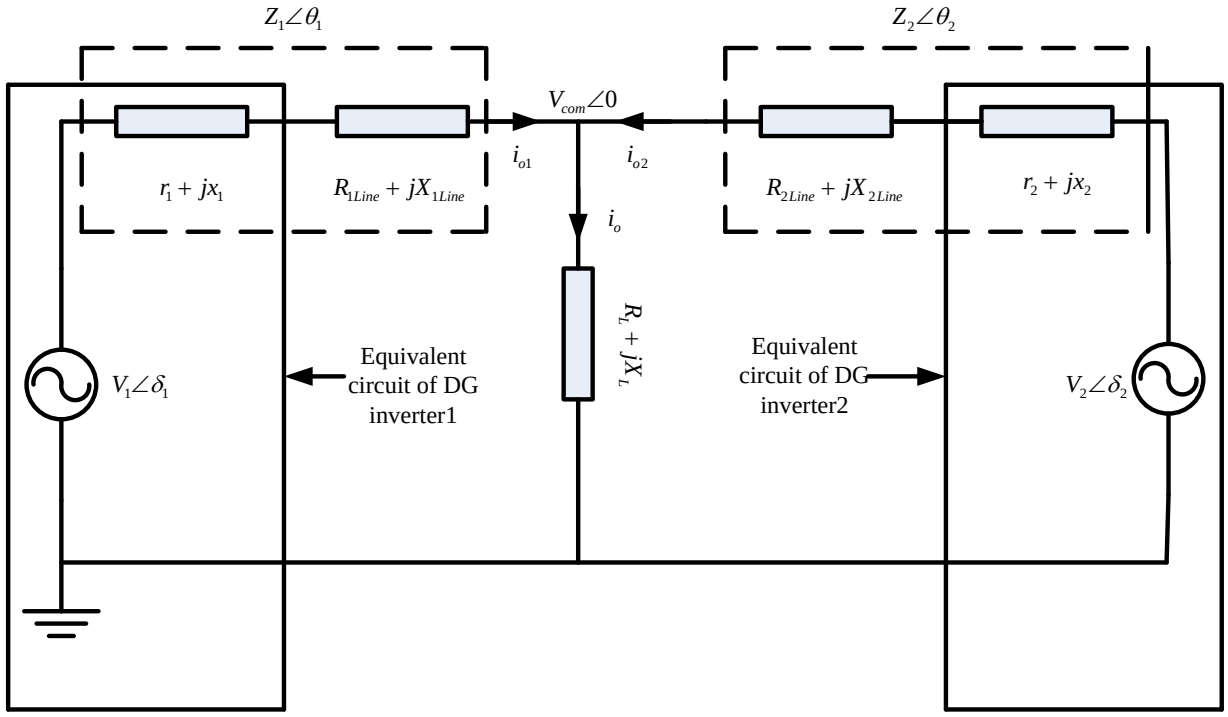

Figure 1: DG Inverters equivalent circuit in autonomous mode.

The DG inverters output current and power is given by:

$$i_i = \frac{V_i\angle\delta_i - V_{com}\angle 0}{Z_i\angle\theta_i}, S_i = V_i\angle\delta_i \times i_i^* = P_i + jQ_i (\mathrm{i} = 1, 2 ..... n) \quad (1)$$

where *n* is the number of DG inverters; P_i and Q_i are the active and reactive power output of the i[th] DG inverter respectively which are expressed as:

$$P_i = \frac{1}{Z_i}[(V_i V_{com}\cos\delta_i - V_{com}^2)\cos\theta_i + V_i V_{com}\sin\delta_i \sin\theta_i] \tag{2}$$

$$Q_i = \frac{1}{Z_i}[(V_i V_{com}\cos\delta_i - V_{com}^2)\sin\theta_i - V_i V_{com}\sin\delta_i \cos\theta_i] \tag{3}$$

When the sum of output impedance and line impedance is purely inductive, $\theta_i = 90^\circ$, so the equations (2) and (3) are simplified as:

$$P_i = \frac{V_i V_{com}}{X_{iLine}}\delta_i \tag{4}$$

$$Q_i = \frac{V_i V_{com} - V_{com}^2}{X_{iLine}} \tag{5}$$

From equations (4) and (5), it is clear that the power angle δ_i determines the flow of active power, whereas, voltage amplitude V_{com} determines the flow of reactive power. Voltage phase angle δ_i and active power, voltage amplitude V_{com} and reactive power, have linear relationship. The *P-f/Q-V* droop control curve is shown in Fig. 2(a) and control equations are given by [10], [11], [27]:

$$f_i = f_i^* - m_i(P_i - P_i^*) \tag{6}$$

$$V_i = V_i^* - n_i(Q_i - Q_i^*) \tag{7}$$

where f_i^* and V_i^* are the voltage amplitude and frequency of the DG inverters output; m_i, n_i are the *P-f/Q-V* control coefficients; P_i^* and Q_i^* are respectively the rated active and reactive power of the i[th] DG inverter output.

Similarly, when the sum of output impedance and line impedance is purely resistive, $\theta = 0$, equations (2) and (3) are simplified and the *P-V/Q-f* droop control curve is as shown in Fig. 2(b). The control equations are given by [14], [29]:

$$f_i = f_i^* + n_i(Q_i - Q_i^*) \tag{8}$$

$$V_i = V_i^* - m_i(P_i - P_i^*) \tag{9}$$

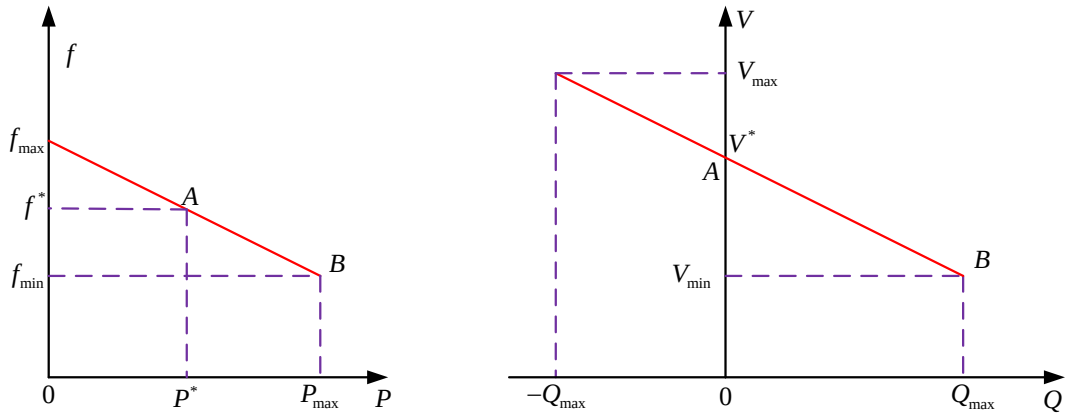

(a) *P-f/Q-V* Droop control curve.

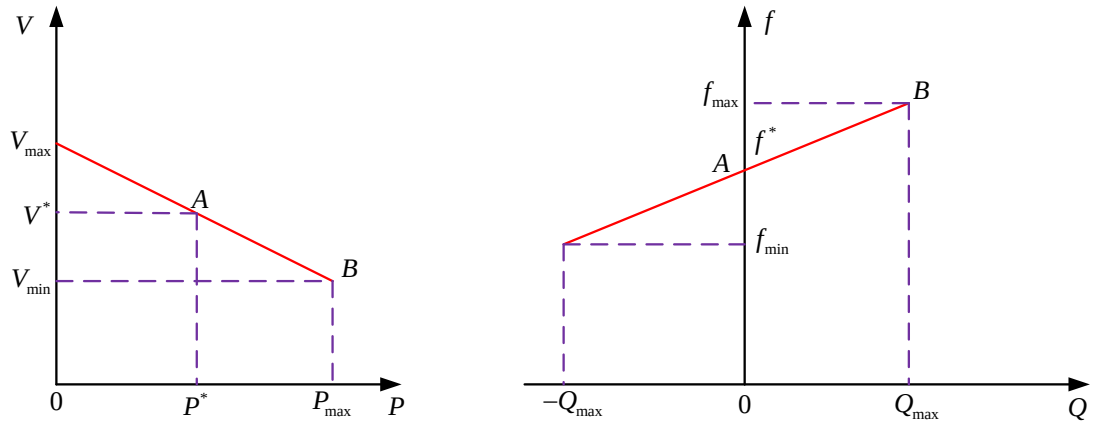

(b) *P-V/Q-f* Droop control curve.

$P_{max,i}$ and $Q_{max,i}$: Maximum allowable active and reactive power of the DG inverter.

$f_{max,i}$ and $V_{max,i}$: Maximum output frequency and output voltage amplitude of the DG inverter.

$f_{min,i}$ and $V_{min,i}$: Minimum frequency and voltage amplitude allowed by the DG inverter.

Figure 2: Droop control characteristics.

2.2 Power distribution condition between DG inverters

When the parallel DG inverters is operated in isolated mode, the output frequency and voltage of each DG inverter is the same [30], [31]. The droop control method to achieve a reasonable distribution of the load power, needs to meet the following equations.

$$m_1 P_1^* = m_2 P_2^*, n_1 Q_1^* = n_2 Q_2^*, f_1^* = f_2^*, V_1^* = V_2^* \tag{10}$$

$$\delta_1 = \delta_2, \frac{X_{1Line}}{m_1} = \frac{X_{2Line}}{m_2}, V_1 = V_2, \frac{X_{1Line}}{n_1} = \frac{X_{2Line}}{n_2} \tag{11}$$

$$n_1P_1^* = n_2P_2^*, m_1Q_1^* = m_2Q_2^*, f_1^* = f_2^*, V_1^* = V_2^* \tag{12}$$

$$V_1 = V_2, \frac{R_{1Line}}{n_1} = \frac{R_{2Line}}{n_2}, \delta_1 = \delta_2, \frac{R_{1Line}}{m_1} = \frac{R_{2Line}}{m_2} \tag{13}$$

Equations (10), (11), (12) and (13) show that, to realize the proportional sharing of active and reactive power of parallel DG inverters, it is necessary to satisfy the following conditions.

1) Each DG inverter droop coefficients should be inversely proportional to the rated capacity.

2) Each parallel DG inverter voltage and frequency should match to the rated value.

3) The output voltage of each DG inverter should have same amplitude and phase.

4) The line impedance at the output of each DG inverter is inversely proportional to droop coefficients [29], [31].

In a microgrid system, the above is the condition of power sharing between DG inverters under the inductive and resistive line model. In addition, the output impedance of the inverter and line impedance to the load are different, considering geographical location and other factors, with a certain degree of randomness, it is difficult to satisfy equations (10), (11), (12) and (13) and is difficult to realize the proportional power sharing between the DG inverters according to the *P-f/Q-V, P-V/Q-f* droop control schemes.

3. Microgrid droop control strategy

In a microgrid, a droop control is actually used to simulate the droop characteristics of the synchronous generator to adjust the voltage and frequency of the DG inverters output, so that the micro-grid can operate under different load requirements. As can be seen from Fig. 3, where L is the filter inductor, C is the filter capacitor, r is the filter inductor equivalent resistance and Z_{Load} is the load impedance, the droop control model of microgrid can be divided into two parts: voltage and current loop control model and power droop control model. First, the output voltage and current of the micro-power supply are obtained by sampling the DG inverter module. The output power of the micro-power supply is obtained by the power calculation unit and the low-pass filter, and then calculated according to the active power droop controller and the reactive power droop controller respectively. The reference voltage values V_{dref} and V_{qref} is finally adjusted by the voltage PI control and i_{dref} and i_{qref} are adjusted by the current P control to obtain controllable sinusoidal modulation signal m to the DG inverter.

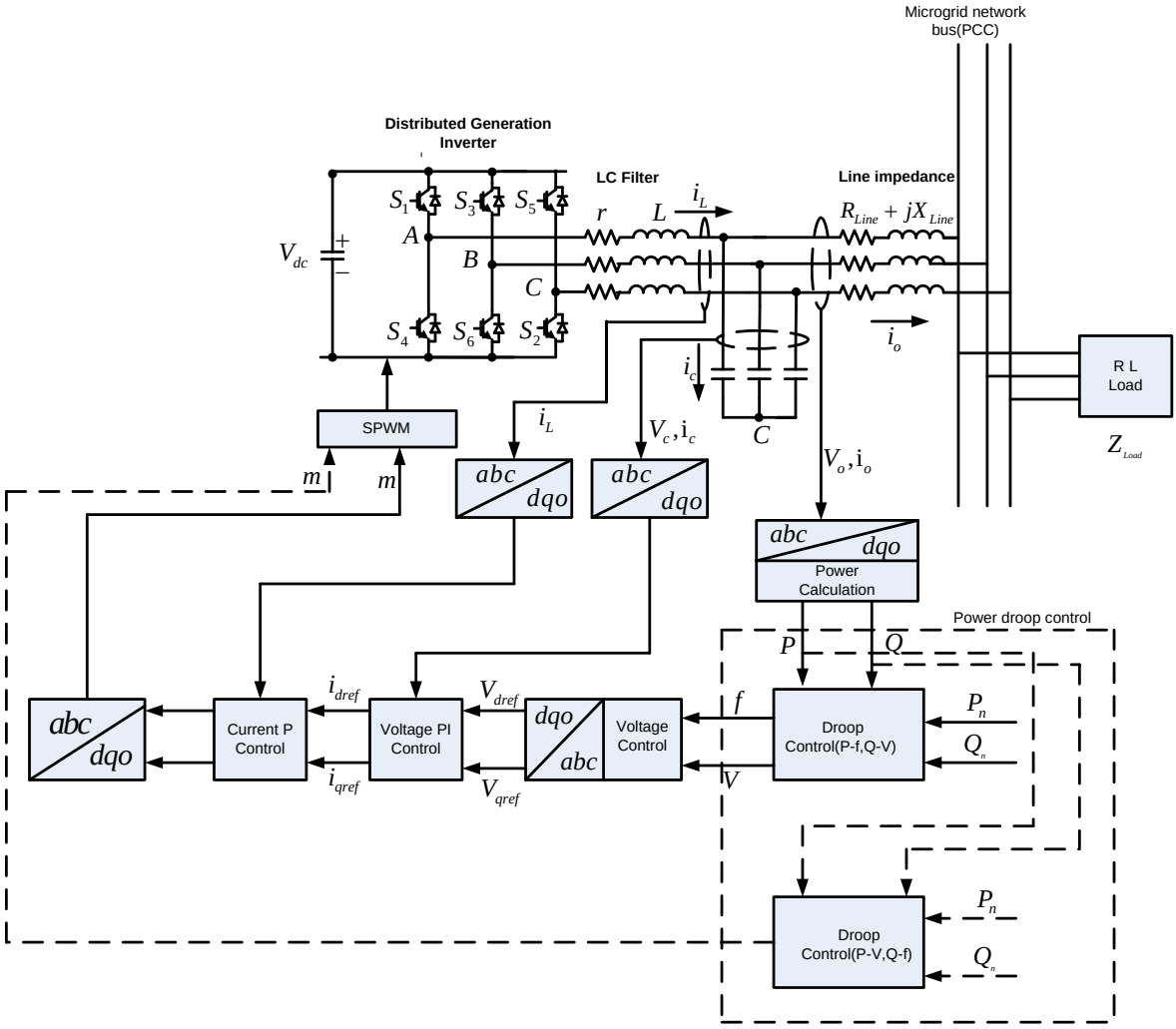

Figure 3: Droop control block diagram.

3.1 Voltage and current dual loop control of DG inverters

Voltage and current dual-loop control [21] is the main inverter control strategy as shown in Fig. 4, in which the current inner loop improves system stability, system dynamic response and damping properties. The inner current loop feedback is of two types, capacitor current mode [26], [31] and inductor current mode [30]. As compared to the inductor current mode feedback, the feedback capacitor current mode provides better noise immunity, but is unable to carry out inverter current limit protection. Research in [21] have shown that, for larger values of current controller proportional parameter K_{pi}, better dynamic response of the current loop is achieved. But, if K_{pi} is too large, there is a deterioration in the system stability. On the other hand, the smaller values of voltage controller parameter K_{pv}, the DG inverter output impedance is resistive. If K_{pv} takes larger values, the DG inverter output impedance is inductive. Similarly, the selection of the integral parameter K_{vi} has a significant effect on the characteristics of the inverter output impedance. In other words, the steady-state as well as the dynamic characteristics

of DG inverter output depends on the parameter design of the controller. When the control parameter is a fixed value, it is difficult to meet the microgrid island operation in adjusting the voltage amplitude and frequency, during the changes in power supply fluctuations. Therefore, it is necessary to control the use of reasonable structure and parameter tuning method to achieve stable control of microgrid in islanding mode. In Fig. 4-5, V_{ref} is the voltage loop reference, V_0 is the inverter output voltage, K_{PWM} is the gain of the three phase full bridge circuit, $G_v(s)$ and $G_i(s)$ respectively are the voltage loop and current loop controllers, i_0 is the output current of the inverter and i_c is the capacitive feedback signal.

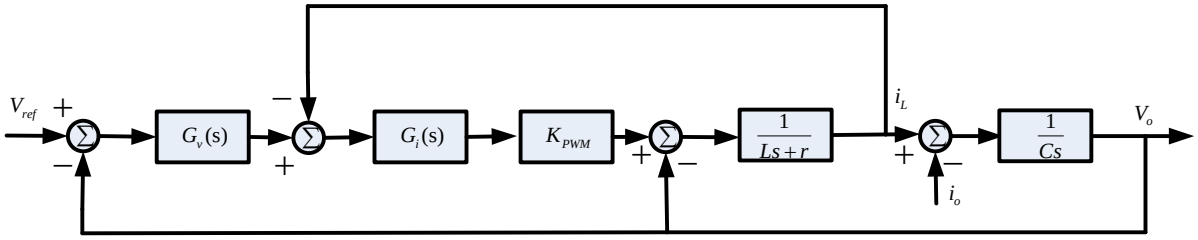

Figure 4: Voltage and current dual loop control block diagram.

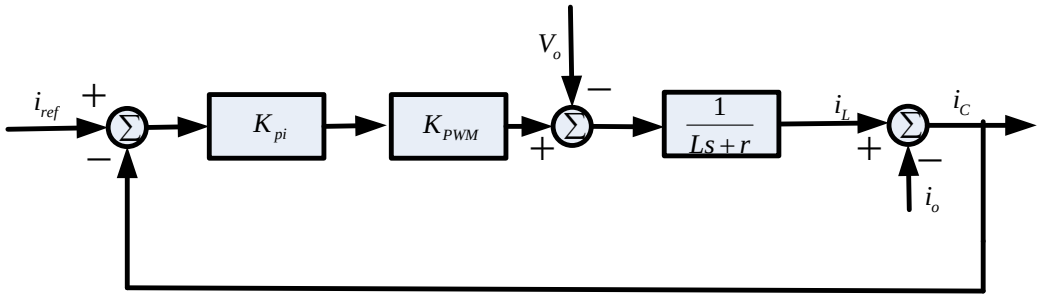

Figure 5: Current loop block diagram.

To make sure the inner current loop has a better tracking performance under different load conditions, the inner current loop cut off frequency is chosen as $f_{ib} = \frac{1}{5} f_s$ [31]. The impact of the load current i_o is neglected. Current loop closed loop block diagram is as shown in Fig. 5 and the transfer function is given by:

$$\mathrm{G}_i(s) = \frac{i_c(s)}{i_{ref}(s)} = \frac{G_i(s)K_{PWM}}{Ls + r + G_i(\mathrm{s})\,\mathrm{K}_{PWM}} \tag{14}$$

From equation (14) the amplitude frequency characteristics of the transfer function is:

$$\left|G_i(j\omega)\right| = \frac{K_{pi}K_{PWM}}{\sqrt{\omega^2 L^2 + (K_{pi}K_{PWM} + r)^2}} \tag{15}$$

Current loop control parameter $K_{pi} = 2.5$ is obtained from the bode diagram as shown in Fig. 6.

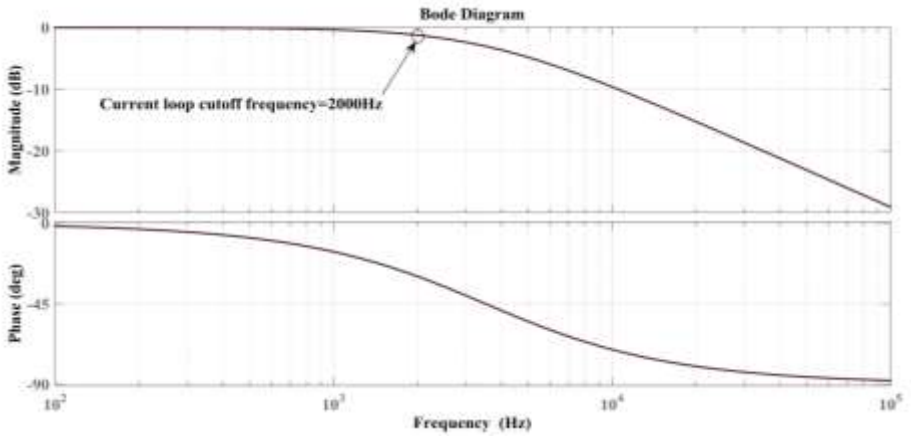

Figure 6: Bode diagram of the current loop.

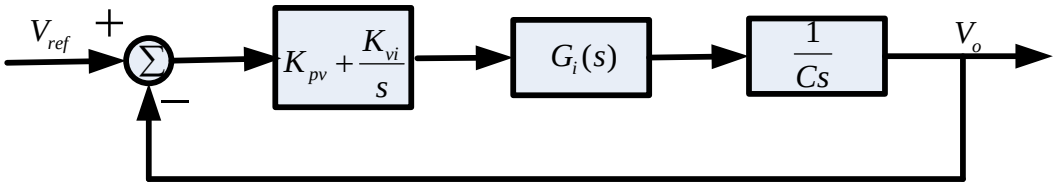

Figure 7: Voltage loop block diagram.

In order to avoid mutual coupling on the voltage loop and current loop, the cut off frequency of the voltage loop should be less than half of the current loop bandwidth. Hence, voltage loop cutoff frequency is chosen as 800 Hz [31]. From the voltage loop closed loop block diagram as shown in the Fig. 7, the transfer function is obtained as:

$$G_V(s) = \frac{(K_{pv} + \frac{K_{vi}}{s})G_i(s)}{Cs + (K_{pv} + \frac{K_{vi}}{s})G_i(s)} \tag{16}$$

In equation (16), at first, integral coefficient K_{vi} is set to 0; the outer voltage cut-off frequency is set to 800 Hz; K_{pv} is obtained as 0.6. In order to ensure that the system bandwidth

is within the required range, the selected system bandwidth is f_{vb} = 810 Hz, then K_{vi} =290 is obtained. Voltage loop bode diagram as shown in the Fig. 8.

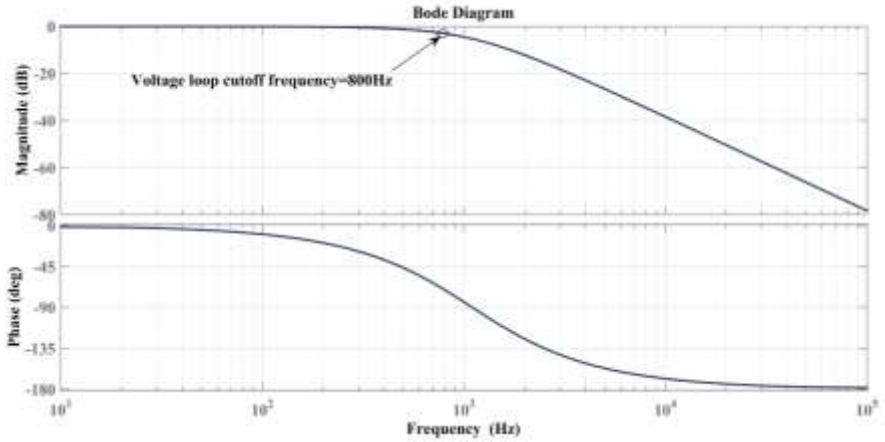

Figure 8: Bode diagram of the voltage loop.

The inverter output impedance transfer function is given by:

$$Z_o(s) = \frac{A_1 s^2 + A_2 s}{A_3 s^3 + A_4 s^2 + A_5 s + A_6} \tag{17}$$

$$A_1 = L, A_2 = r + K_{pi}K_{pwm}, A_3 = LC, A_4 = K_{pi}K_{pwm}C + rC,$$
$$A_5 = K_{pi}K_{pwm}K_{pv} + 1, A_6 = K_{pi}K_{pwm}K_{vi}. \tag{18}$$

Due to the presence of the output filter inductor and inductive components of the device parameters, the equivalent output impedance of the inverter is generally considered inductive. But, equivalent output impedance of the closed loop of inverter has a relationship with control strategy adopted [22], [27] by adjusting the inverter control parameters. The equivalent output impedance of the DG inverters can be changed to resistive or inductive.

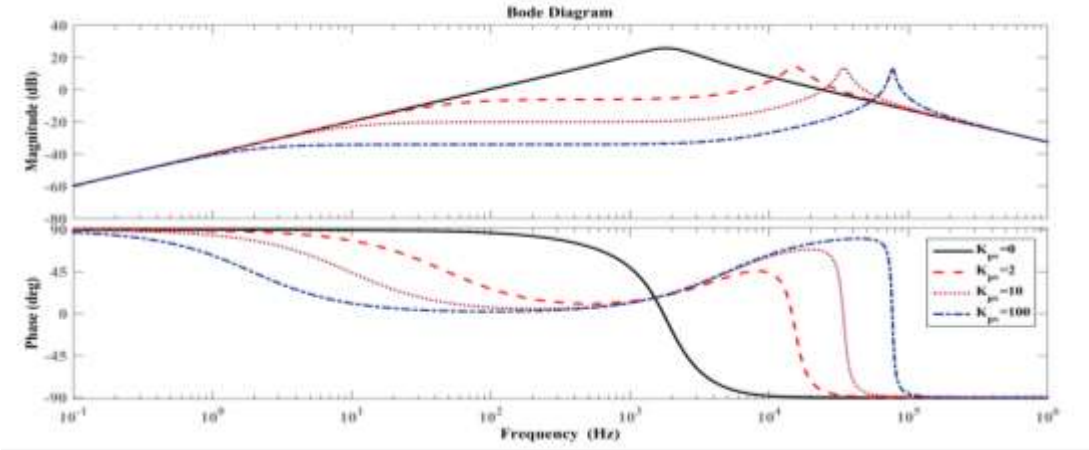

(a) Bode diagram of inverter output impedance with different K_{pv}.

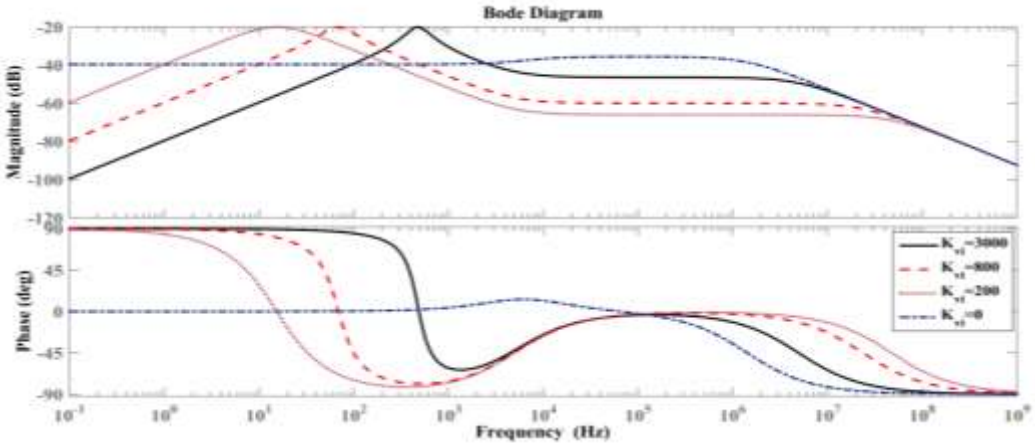

(b) Bode diagram of inverter output impedance with different K_{vi}.

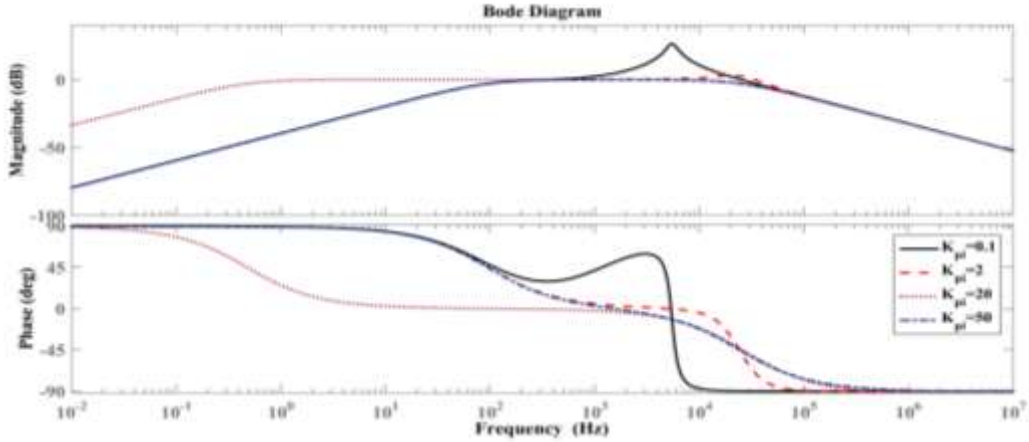

(c) Bode diagram of inverter output impedance with different K_{pi}.

Figure 9: Bode diagram of inverter output impedance with different parameters variation K_{pv}, K_{vi} and K_{pi}.

Fig. 9(a) shows that the voltage loop proportional factor has some influence on the DG inverter output impedance. When $K_{pv} = 0$, the inverter output impedance at 50 Hz is more inductive. With the increasing K_{pv} value the DG inverter output impedance at 50 Hz is more resistive.

Fig. 9(b) shows that the voltage loop integral factor has some influence on the inverter output impedance. When K_{vi} =0, the inverter output impedance at 50 Hz is approximately more resistive, with increasing K_{vi} the output impedance of the DG inverter at 50 Hz is more capacitive.

Taking K_{pi}=0.1, 2, 20, 50 the DG inverter output impedance at 50 Hz is as shown in Fig. 9(c). The current loop proportional coefficient has little effect on the output impedance nature of DG inverters.

Based on the PI control parameters obtained from the bode diagram in the Fig. 6 and 8, K_{pv}=0.6, K_{vi}=290, K_{pi}=2.5. The output impedance of the DG inverters are calculated using equation (19). The output impedance angle at 50 Hz is 83° as shown in the Fig. 10. In ensuring the stability of the microgrid system, the DG inverters output impedance is approximated as inductive for *P-f/Q-V* droop control and resistive for the *P-V/Q-f* droop control. If the DG inverter closed loop output impedance design is reasonable, it can reduce the impact of line impedance imbalance. Different values of the system parameters of the DG inverters output impedance magnitude and angle has a direct impact on power sharing. To further reduce the effect of DG inverter output impedance and line impedance effect on the parallel DG inverters, virtual resistors and inductors are added to the control loop, so that DG inverter output impedance nature is changed to inductive for the *P-f/Q-V* droop control and resistive for the *P-V/Q-f* droop control.

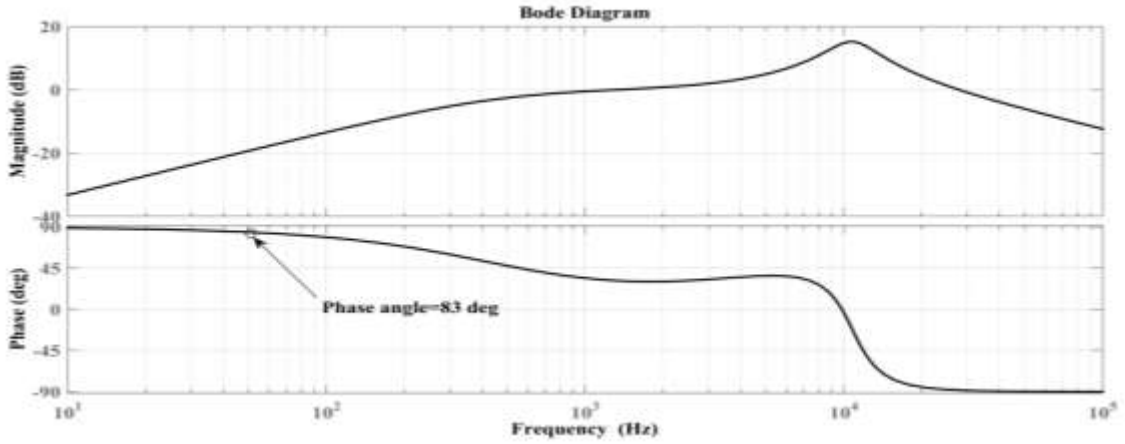

Figure 10: Bode diagram of DG inverter output impedance.

3.2 Virtual impedance design for DG inverters

Virtual impedance control has become a necessary condition for multi voltage source inverter operated in parallel for normal operation in the microgrid system [21], [26]. Equivalent output impedance of the DG inverters is affected by multiple factors, filter parameters, voltage and current control loop parameters, the differences of these factors led to inconsistencies of power sharing between the parallel DG inverters. Virtual impedance block diagram as shown in Fig. 11 and is given by [25], [29].

$$V_{ref} = V_{ref}^{*} - Z_{vir} i_o \tag{19}$$

$$V_o = G_i(s)G_v(s)V_{ref}^* - [G_i(s)G_v(s)Z_{vir}(s) + Z_o(s)]i_o \tag{20}$$

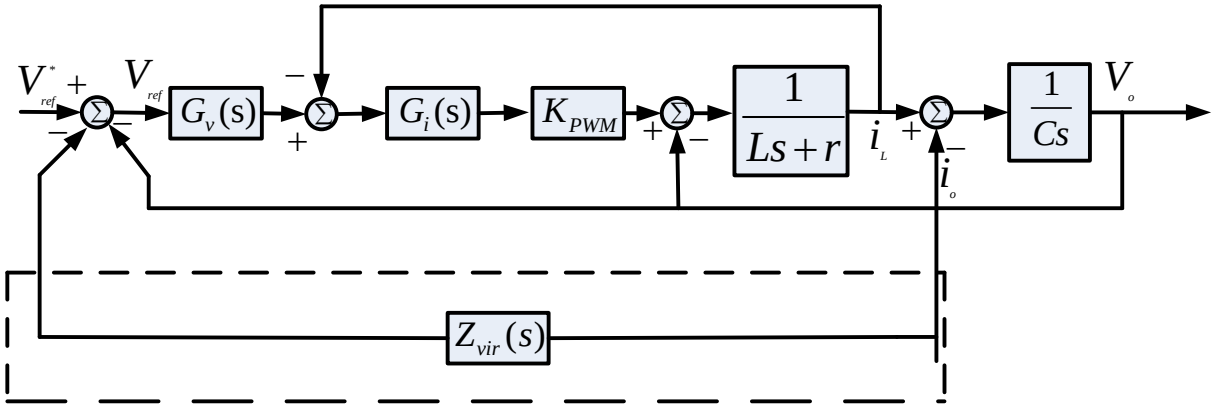

Figure 11: Virtual impedance control block diagram.

Virtual inductor is expressed as [16]:

$$Z_{vir} = sL_v, Z_o(s) = \frac{B_1 s^2 + B_2 s}{B_3 s^3 + B_4 s^2 + B_5 s + B_6} \tag{21}$$

$$\begin{aligned} B_1 &= L + L_v K_{pi} K_{pwm} K_{pv} \\ B_2 &= r + K_{pi} K_{pwm} + L_v K_{pi} K_{pwm} K_{vi} \\ B_3 &= LC, B_4 = K_{pi} K_{pwm} C + rc \\ B_5 &= K_{pi} K_{pwm} K_{vi} \\ B_6 &= K_{pi} K_{pwm} K_{vi} \end{aligned} \tag{22}$$

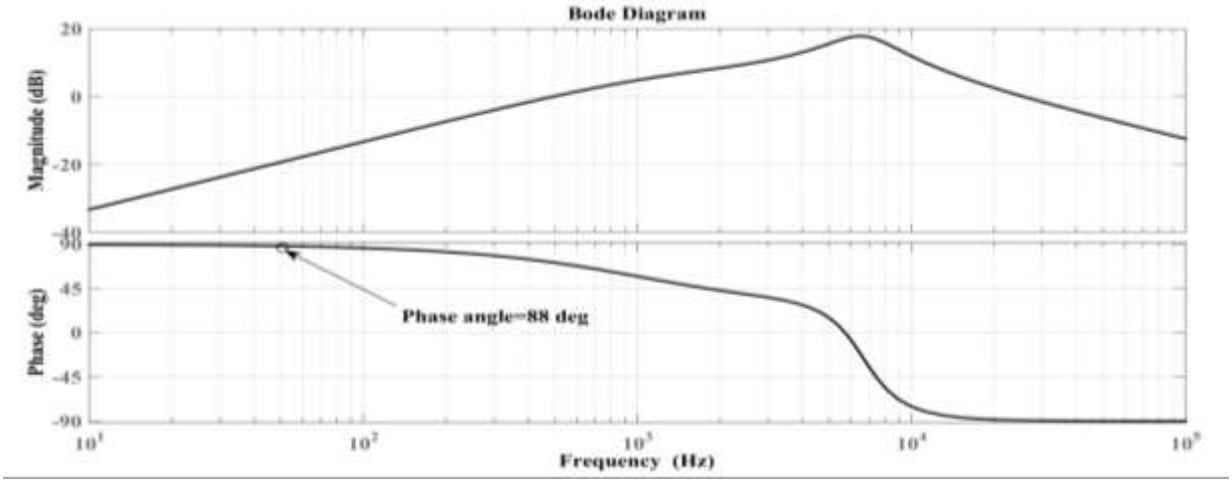

Figure 12: Bode diagram of inverter output impedance with virtual inductor.

If the line impedance is inductive, virtual inductors are added the control loop of the *P-f/Q-V* droop control to improve the power decoupling effect. Impedance angle at 50 Hz is 88° as shown in the Fig. 12. The parallel inverter output impedance tends to more inductive, which has a major role in improving the power sharing.

Virtual resistor is expressed as [29]:

$$Z_{vir}(s) = R_v, Z_o(s) = \frac{C_1 s^2 + C_2 s + C_3}{C_4 s^3 + C_5 s^2 + C_6 s + C_7} \tag{23}$$

$$\begin{aligned} &C_1 = L, C_2 = r + K_{pi} K_{pwm} K_{pv} R_v, C_3 = R_v K_{pi} K_{pwm} K_{vi}, C_4 = LC \\ &C_5 = rC + K_{pi} K_{pwm} C, C_6 = 1 + K_{pi} K_{pwm} K_{vi}, C_7 = K_{pi} K_{pwm} K_{vi} \end{aligned} \tag{24}$$

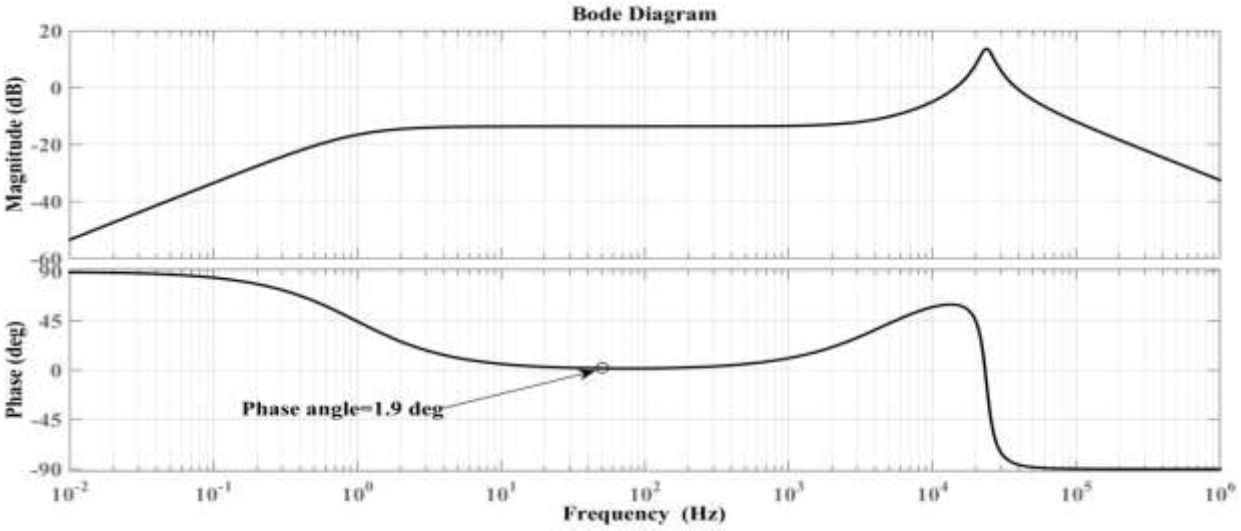

Figure 13: Bode diagram of inverter output impedance with virtual resistor.

If the line impedance is resistive, virtual resistor is added the control loop of *P-V/Q-f* droop control to improve the power decoupling effect. Impedance angle at 50 Hz is 1.9° as shown in the Fig. 13. The parallel inverter output impedance tend to be more resistive, which has a major role in improving the power sharing.

3.3 Droop controllers with frequency and voltage restoration secondary control

In the island type microgrids with traditional *P-f/Q-V* and*P-V/Q-f* droop control, when the load power fluctuates, the output voltage and frequency of the inverter will have a large deviation. Virtual impedance control provides decoupling of active and reactive power for parallel DG inverters, but the virtual impedance method inevitably leads to a voltage drop in the microgrid system. In order to ensure the quality of the voltage and high precision distribution of

active and reactive power, the introduction of voltage, frequency and active power secondary adjustment, so that the voltage and frequency to maintain the rated output, active and reactive power reasonable distribution. Each inverter unit includes reverse droop control and secondary adjustment, without the need for a central controller, enhancing system stability. When the load active power increase to cause the voltage amplitude drop, through the voltage secondary adjustment control to restore the voltage to the rated value. When the load reactive power increase to cause the frequency to decrease, the frequency is restored to the rated value by the frequency adjustment.

Voltage amplitude and frequency variations of DG inverters is improved by proposing secondary control for *P-f/Q-V* and *P-V/Q-f* droop control as shown in the Fig.14-15. The introduction of the feedback link to achieve the inverter output frequency and voltage amplitude compensation, so as to improve the system adaptability and stability [17]. The expression for *P-f/Q-V* droop control is given by:

$$f - f_i = \frac{m_i}{1 - m_i^* \dfrac{K_{ap}s + K_{ai}}{s}}(P_i - P) \tag{25}$$

$$V - V_o = -\frac{n_i}{1 + n_i^* \dfrac{K_{ap}s + K_{ai}}{s}} Q_i \tag{26}$$

The expression for *P-V/Q-f* droop control is given by:

$$V - V_o = \frac{n_i}{1 + n_i^* \dfrac{K_{bp}s + K_{bi}}{s}}(P_i - P) \tag{27}$$

$$f - f_i = \frac{m_i}{1 - m_i^* \dfrac{K_{bp}s + K_{bi}}{s}} Q_i \tag{28}$$

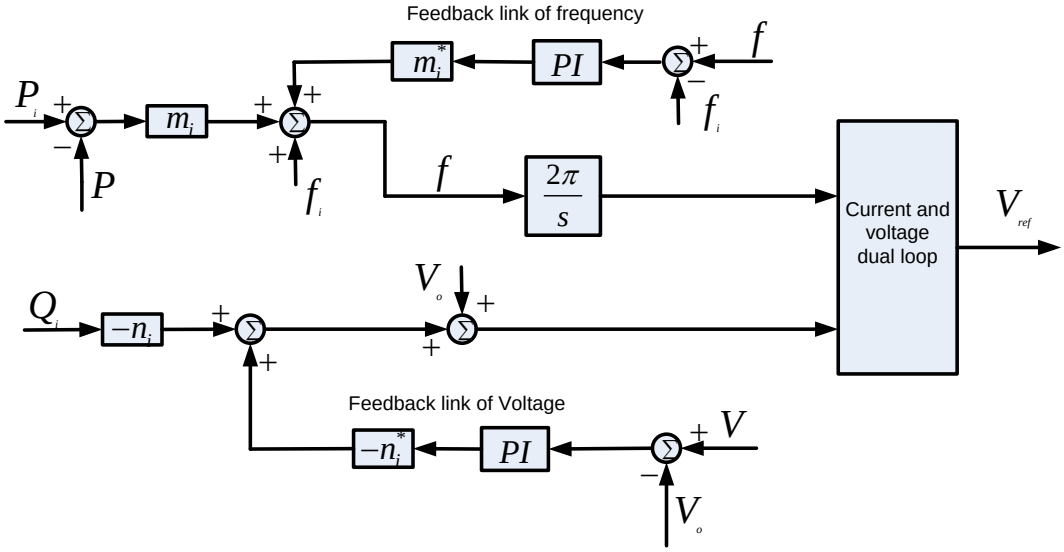

Figure 14: Block diagram of secondary control with *P-f/Q-V* droop control.

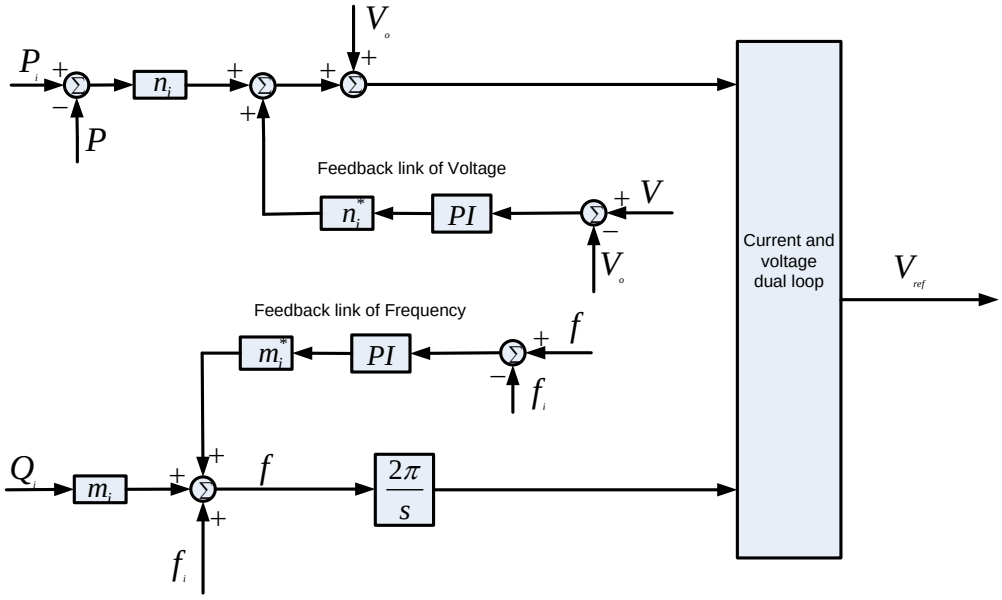

Figure 15: Block diagram of secondary control with *P-V/Q-f* droop control.

In equations (6), (7), (8) and (9), the frequency difference $f - f_i$ and the voltage difference $V - V_o$ as the feedback signal with PI control to modify the *P-f/Q-V* and *P-V/Q-f* droop coefficients of the feedback line to form a improved droop control method. Adjusting the proportional coefficient K_{ap}, K_{bp} and the integral coefficient K_{ia}, K_{ib} of the PI control to

compensate the influence of the output voltage variation of the parallel DG inverters in microgrid. The coefficients m_i^* and n_i^* are the amplification correction droop coefficients, mainly to amplify the feedback part of the voltage and frequency compensation, because the original feedback coefficient m_i and n_i are too small.

4. Simulation Results

In this section, two simulation models of distributed generation inverters connected in parallel are built to verify the proposed *P-f/Q-V* and *P-V/Q-f* improved droop control strategy with resistive and inductive line impedance to ensure the rational allocation of power between parallel inverters. The simulation parameters are shown in the Table 1 (Refer Appendix A).

Case 1:Power sharing analysis of *P-f/Q-V,P-V/Q-f* droop control under resistive line impedance.

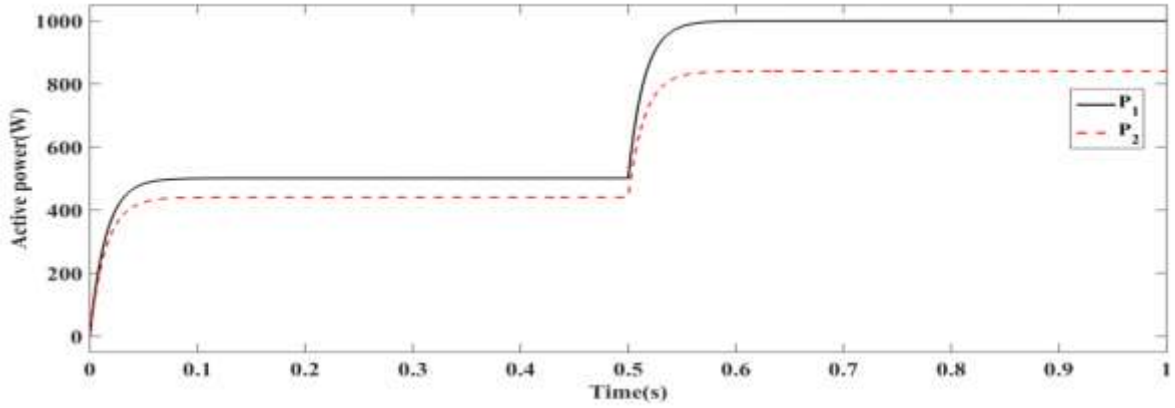

Figure 16: Active power sharing using *P-f/Q-V* droop control under resistive line impedance.

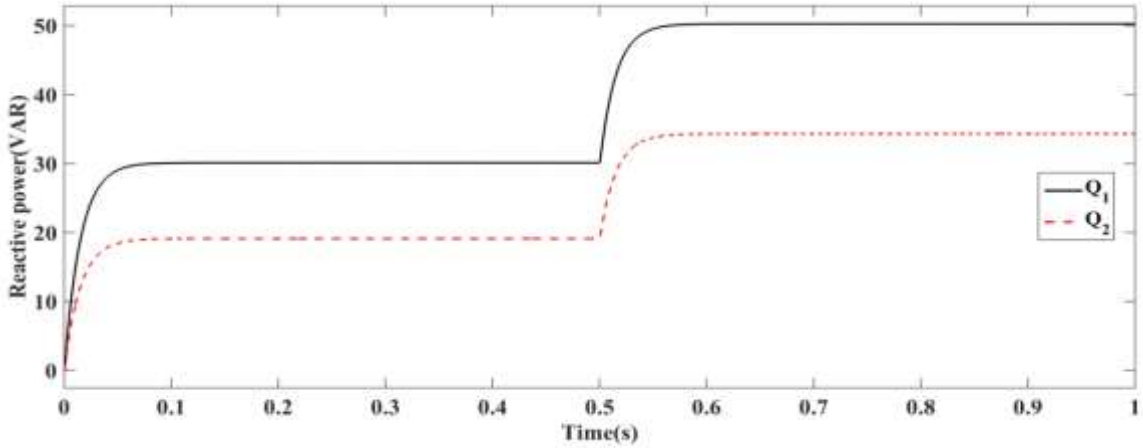

Figure 17: Reactive power sharing using *P-f/Q-V* droop control under resistive line impedance.

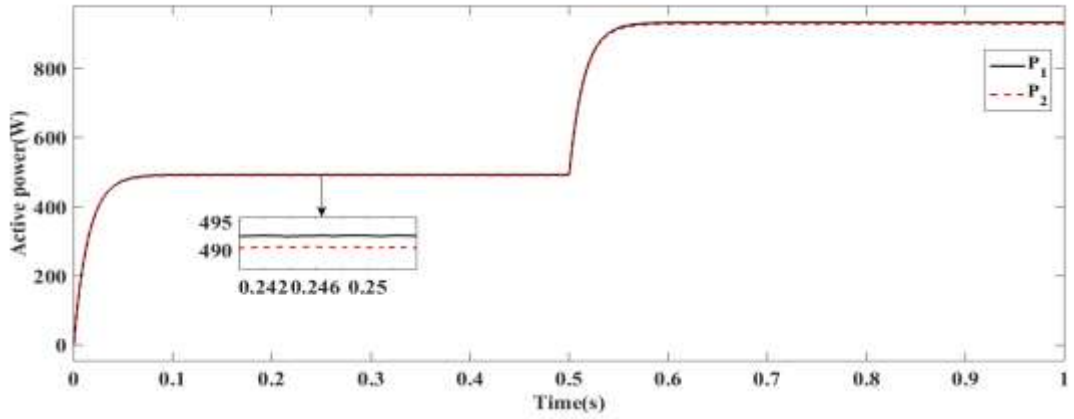

Figure 18: Active power sharing using *P-V/Q-f* droop control with virtual resistor under resistive line impedance.

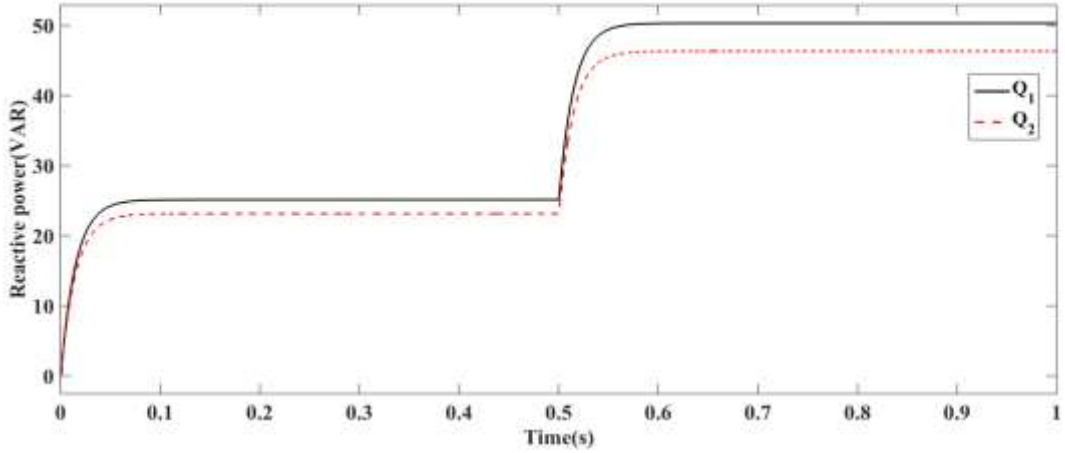

Figure 19: Reactive power sharing using *P-V/Q-f* droop control with virtual resistor under resistive line impedance.

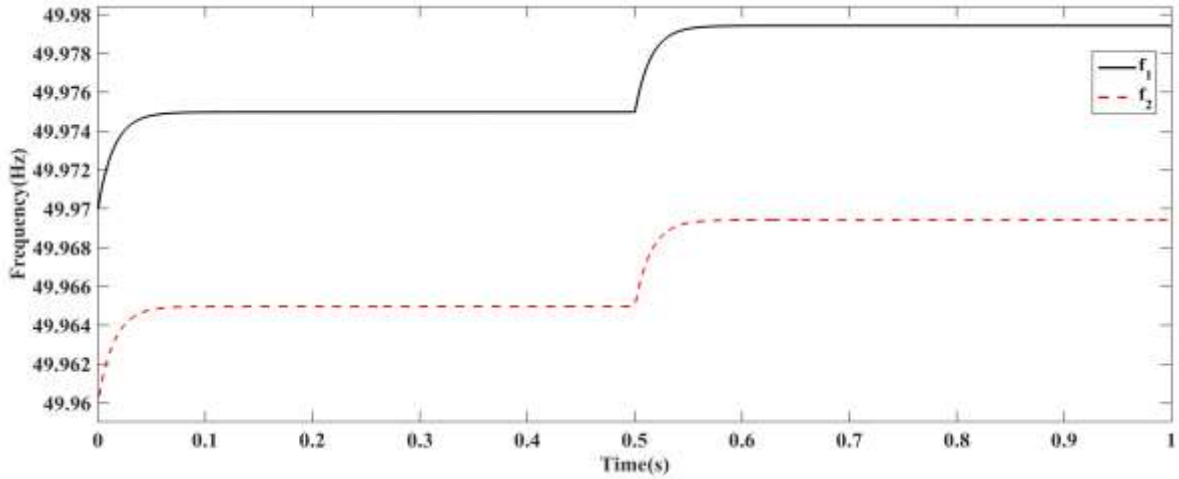

Figure 20: Parallel inverter output frequency using *P-V/Q-f* droop control with virtual resistor under resistive line impedance.

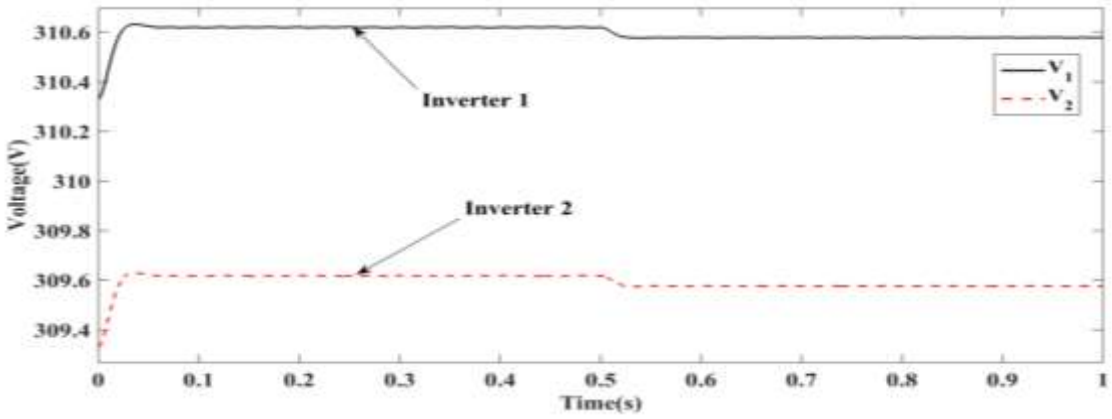

Figure 21: Parallel inverter output voltage using *P-V/Q-f* droop control with virtual resistor under resistive line impedance.

Power sharing of parallel inverters is investigated with common load of P_{load} = 1000 W, Q_{load} = 30 VAR and at 0.5 s sudden local load value of P_{load} = 900 W, Q_{load} = 30 VAR is added to verify the dynamic response and line impedance of $R_{1Line} + jX_{1Line}$ = 0.5+j0.001 Ω, $R_{2Line} + jX_{2Line}$ = 0.6+j0.002 Ω. Initially *P-f/Q-V* droop control is applied to the parallel DG inverters and output power of parallel DG inverters does not reach to a given proportional load sharing, because of the poor decoupling of power as shown in the Fig. 16-17. When the line impedance is resistive *P-f/Q-V* droop control cannot realize the proportional load sharing of active and reactive powers. Now with the same parameters, *P-V/Q-f* droop control based on virtual resistors can reduce the influence of the line impedance difference on the parallel inverters by setting the total output impedance of the DG inverters to be resistive, which improves decoupling of power and realize the proportional load sharing P_1=491 W, P_2=489 W, Q_1=25 VAR, Q_2=23 VAR and at load change at 0.5 s, P_1=932 W, P_2=928 W, Q_1=55 VAR, Q_2=52 VAR as shown in the Fig. 18-19 and frequency variation of DG inverters is within the range of 49.97 Hz to 49.98 Hz, the maximum fluctuation of 0.004 Hz as shown in the Fig. 20. Voltage variation of DG inverters is V_1=310.5 V, V_2=309.5 V as shown in the Fig. 21. Thus, the *P-V/Q-f* droop control with virtual resistors ensures that the voltage change is not greater than 5% and the frequency change is not greater than 1%. This establishes the fact that better accuracy and effectiveness is achieved in the microgrid system.

Case 2: Power sharing analysis of Secondary control with *P-V/Q-f* droop control under resistive line impedance

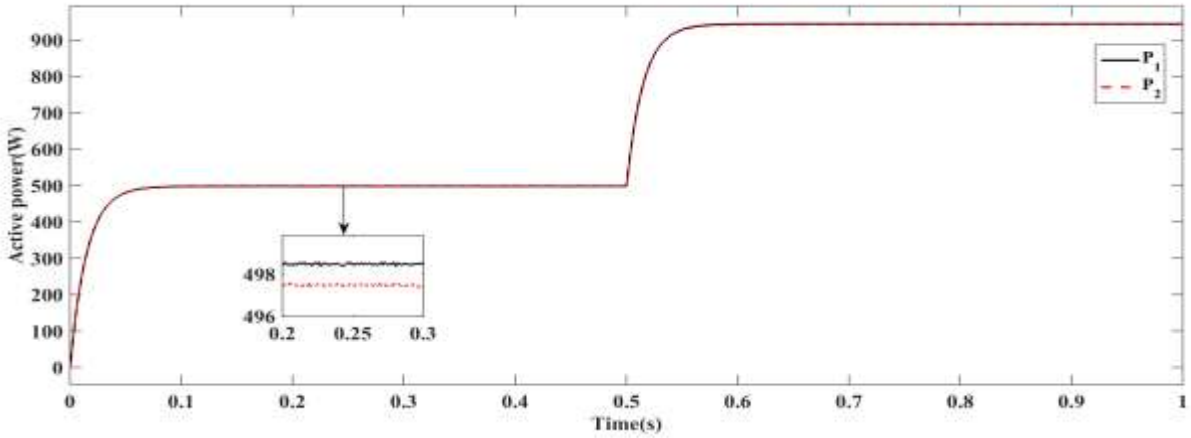

Figure 22: Active power sharing using secondary control with virtual resistor under resistive line impedance.

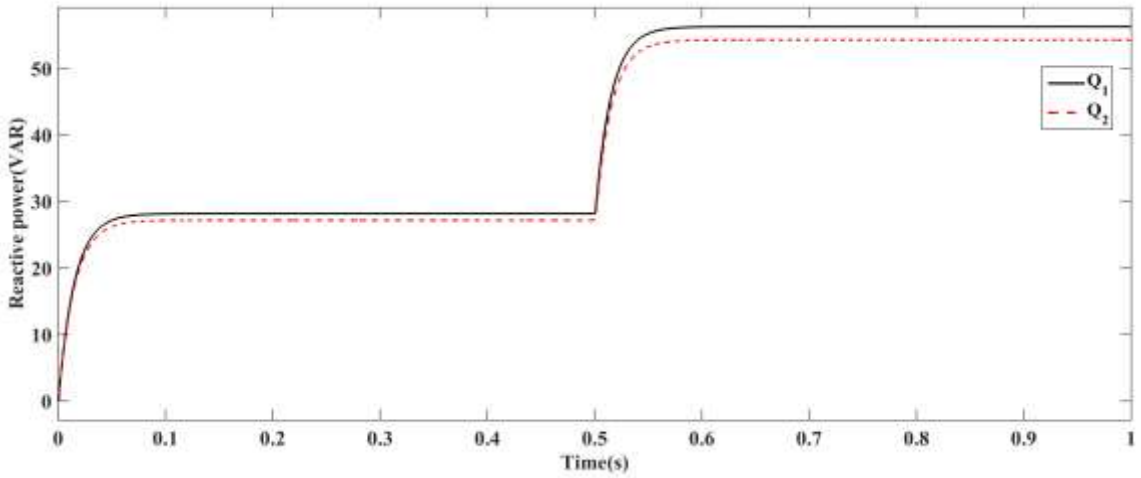

Figure 23: Reactive power sharing using secondary control with virtual resistor under resistive line impedance.

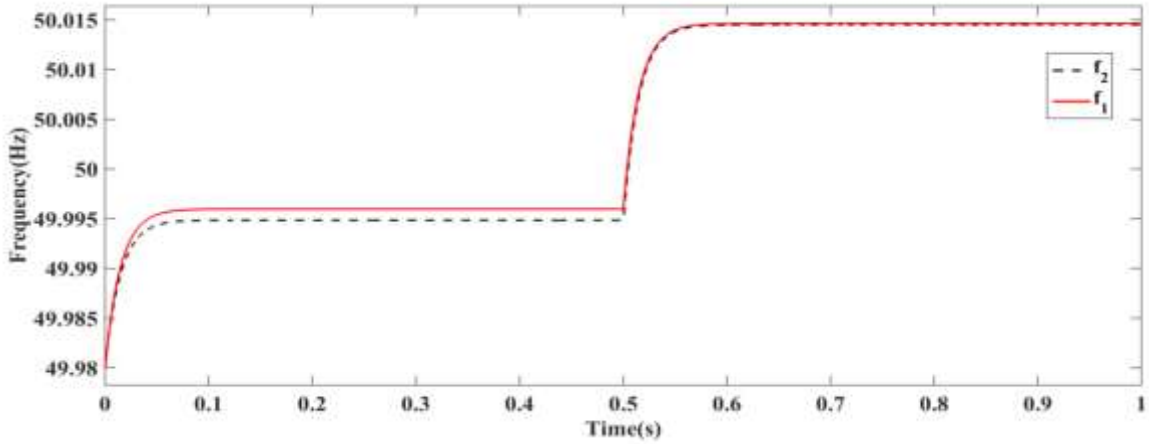

Figure 24: Parallel inverter output frequency using secondary control with virtual resistor under resistive line impedance.

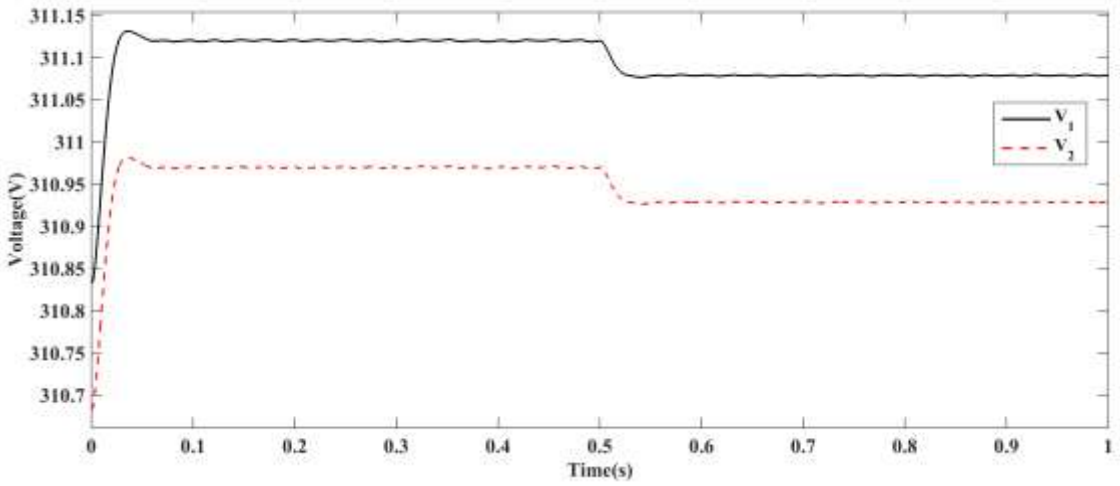

Figure 25: Parallel inverter output voltage using secondary control with virtual resistor under resistive line impedance.

Power sharing of parallel inverters is investigated with common load of P_{load} = 1000 W, Q_{load} = 30 VAR and at 0.5 s sudden local load value of P_{load} = 900 W, Q_{load} = 30 VAR is added to verify the dynamic response and line impedance of $R_{1Line} + jX_{1Line}$ = 0.5+j0.001 $\Omega, R_{2Line} + jX_{2Line}$ = 0.6+j0.002 Ω. *P-V/Q-f* droop control based on virtual resistors with secondary control can reduce the influence of the line impedance difference on the parallel inverters by setting the total output impedance of the DG inverters to be resistive, which improves decoupling of power and improves the proportional load sharing P_1=497 W, P_2=496 W, Q_1=28 VAR, Q_2=27 VAR and at load change at 0.5 s, P_1=943 W, P_2=942 W, Q_1=56 VAR, Q_2=54 VAR as shown in the Fig. 22-23 and frequency variation of DG inverters is within the range of 49.99 Hz to 50.001 Hz, the maximum fluctuation of 0.004 Hz as shown in the Fig. 24. Voltage variation of DG inverters is V_1=311.1 V, V_2=310.9 V as shown in the Fig. 25. Thus, the proposed secondary control for *P-V/Q-f* droop control, ensures voltage amplitude and frequency are restored to the rated value of 50 Hz and 311 V.

Case 3:Power sharing analysis of *P-f/Q-V,P-V/Q-f* droop control under inductive line impedance.

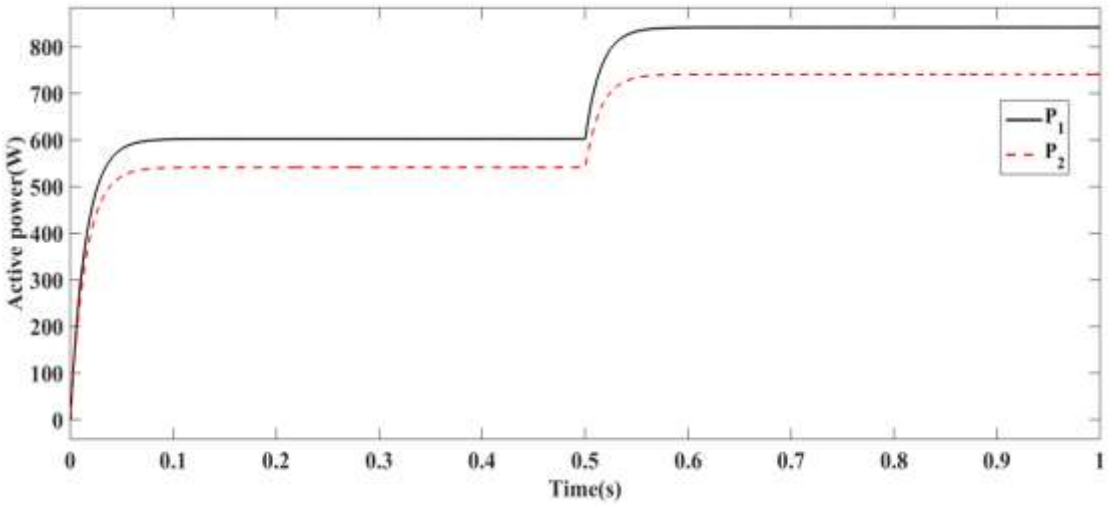

Figure 26: Active power sharing using *P-V/Q-f* droop control under inductive line impedance.

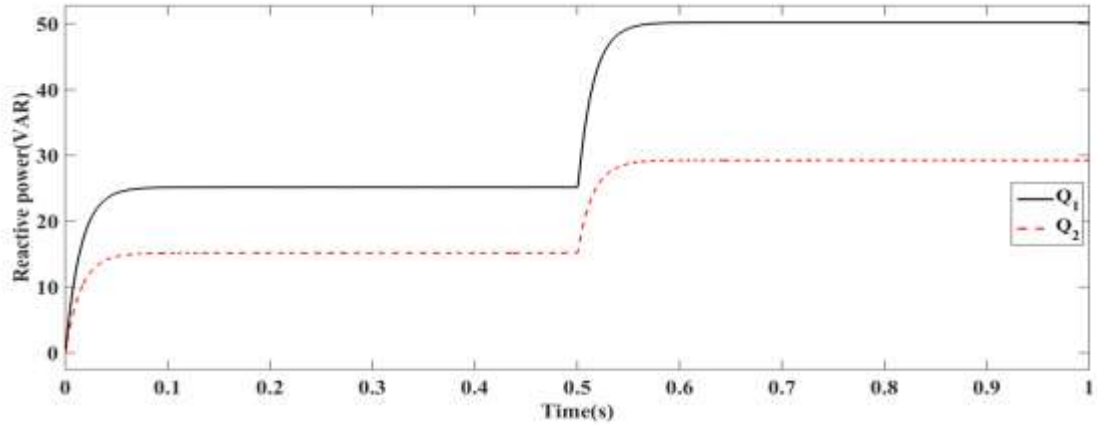

Figure 27: Reactive power sharing using *P-V/Q-f* droop control under inductive line impedance.

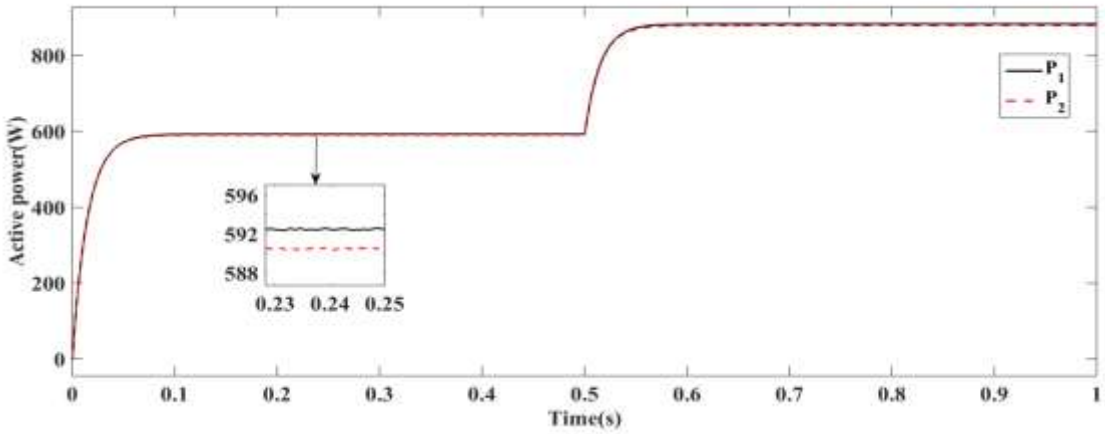

Figure 28: Active power sharing using *P-f/Q-V* droop control with virtual inductor under inductive line impedance.

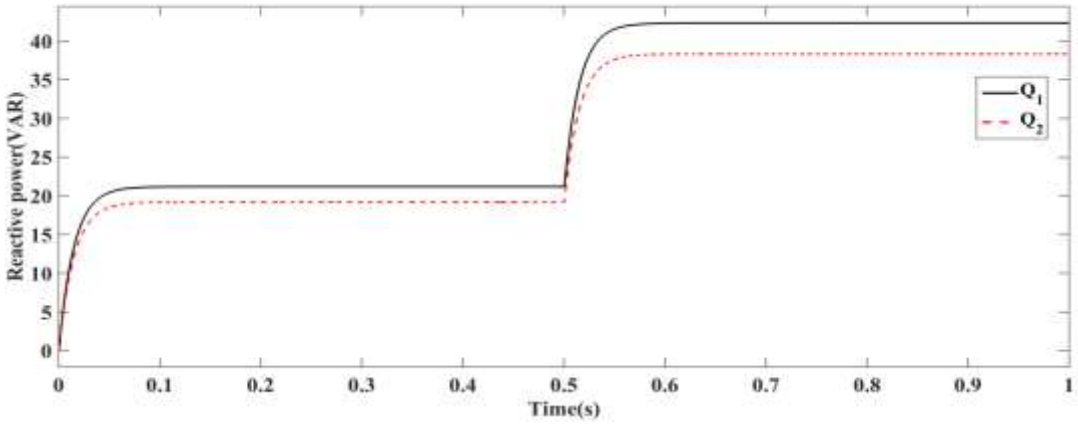

Figure 29: Reactive power sharing using *P-f/Q-V* droop control with virtual inductor under inductive line impedance.

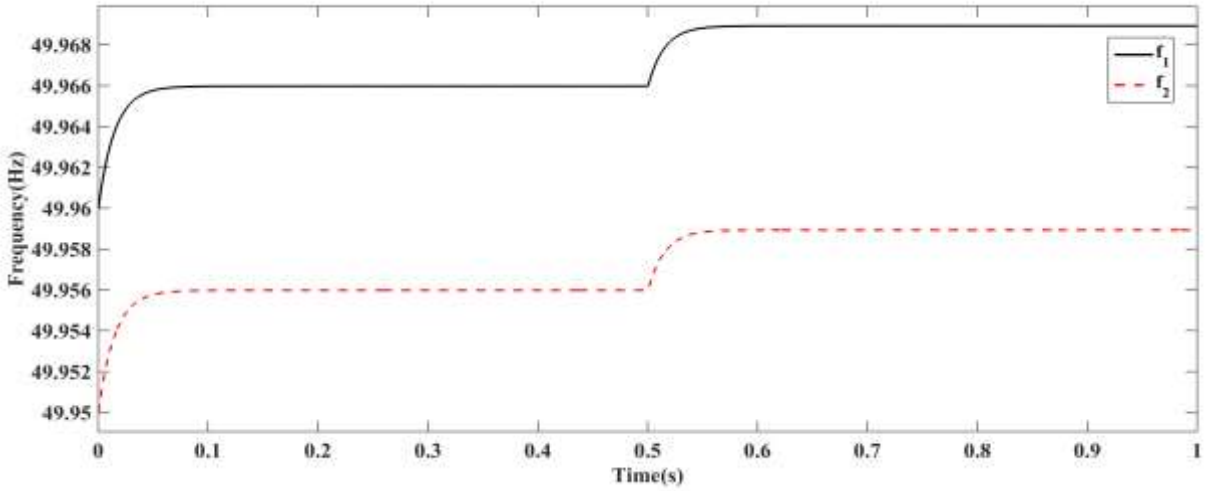

Figure 30: Parallel inverter output frequency using *P-f/Q-V* droop control with virtual inductor under inductive line impedance.

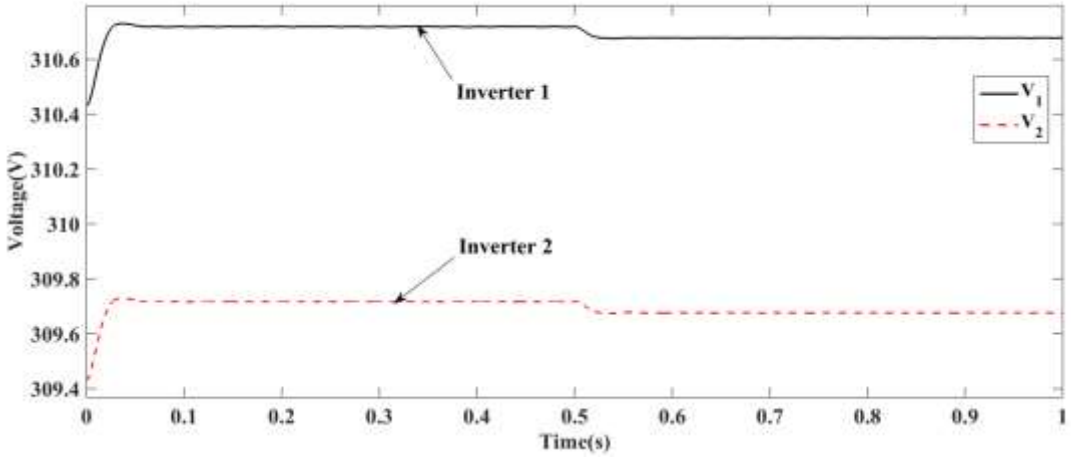

Figure 31: Parallel inverter output voltage using *P-f/Q-V* droop control with virtual inductor under inductive line impedance.

Power sharing of parallel inverters is investigated with common load of P_{load} = 1200 W, Q_{load} = 25 VAR and at 0.5 s sudden local load value of P_{load} = 600 W, Q_{load} = 25 VAR is added to verify the dynamic response and line impedance of $R_{1Line} + jX_{1Line}$ = 0.001+j0.2 Ω, $R_{2Line} + jX_{2Line}$ = 0.002+j0.3 Ω. Initially *P-V/Q-f* droop control is applied to the parallel DG inverters and output power of parallel DG inverters does not reach to a given proportional load sharing, because of the poor decoupling of power as shown in the Fig. 26-27. When the line impedance is inductive *P-V/Q-f* droop control cannot realize the proportional load sharing of active and reactive power. Now with the same parameters *P-f/Q-V* droop control with virtual inductors can reduce the influence of line impedance difference on the parallel DG inverters by setting the total output impedance of the DG inverters to be inductive, which improves decoupling of power and realize the proportional load sharing P_1=591 W, P_2=589 W, Q_1=21VAR, Q_2=19 VAR and at load change at 0.5 s, P_1=882 W, P_2=878 W, Q_1=42 VAR, Q_2=38 VAR as shown in the Fig. 28-29 and frequency variation of DG inverters is within the range of 49.99 Hz to 50.01 Hz, the maximum fluctuation of 0.004 Hz as shown in the Fig. 30. Voltage variation of DG inverters is V_1=310.6 V, V_2=309.6 V as shown in the Fig. 31. Thus, *P-V/Q-f* droop control with virtual inductors ensures that the voltage change is not greater than 5%, the frequency change is not greater than 1% and established a better accuracy and effectiveness in the microgrid system.

Case 4:Power sharing analysis of Secondary control with *P-f/Q-V* droop control under inductive line impedance.

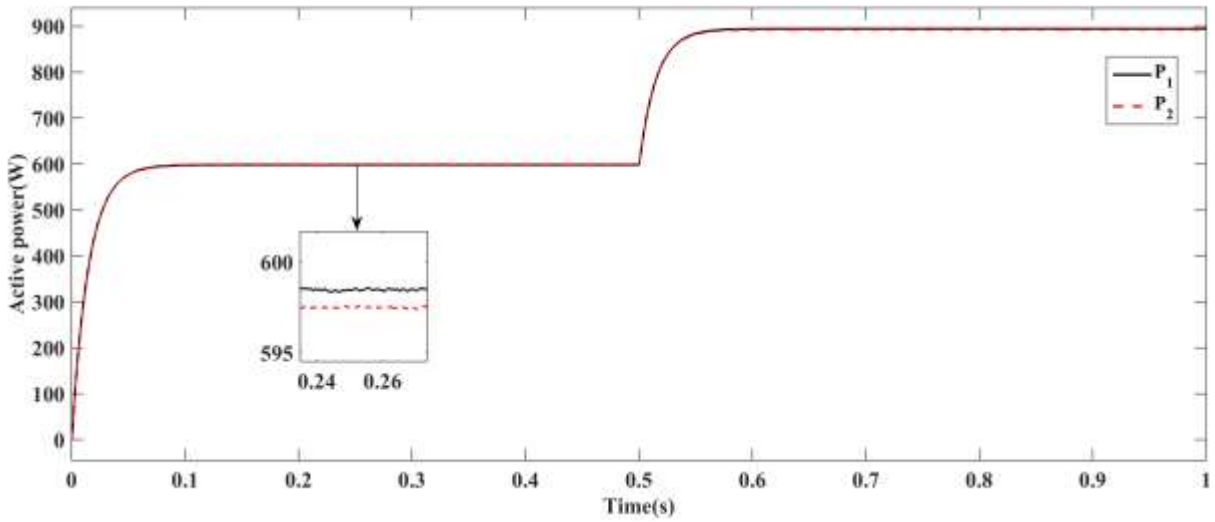

Figure 32: Active power sharing using secondary control with virtual inductor under inductive line impedance.

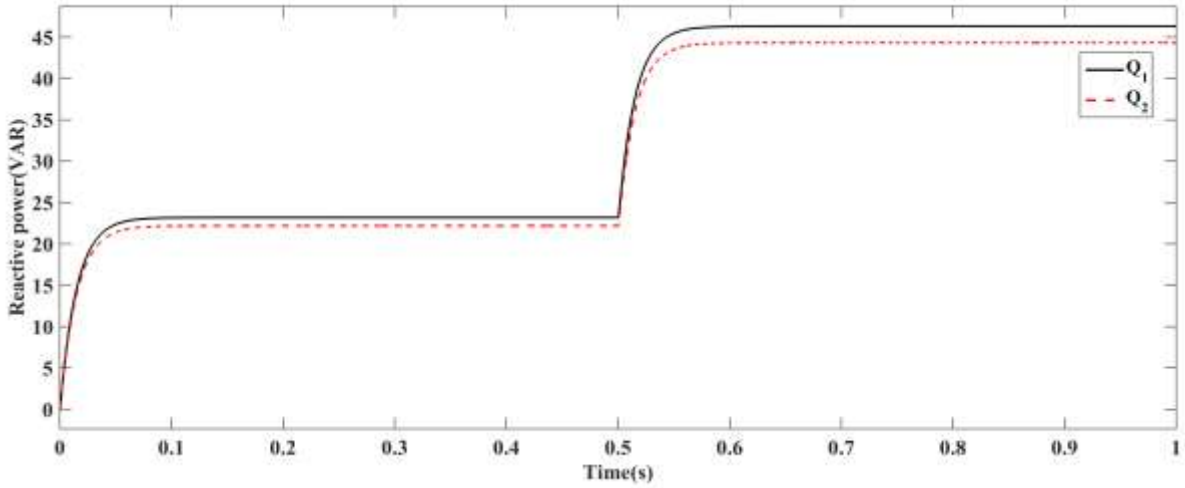

Figure 33: Reactive power sharing using secondary control with virtual inductor under inductive line impedance.

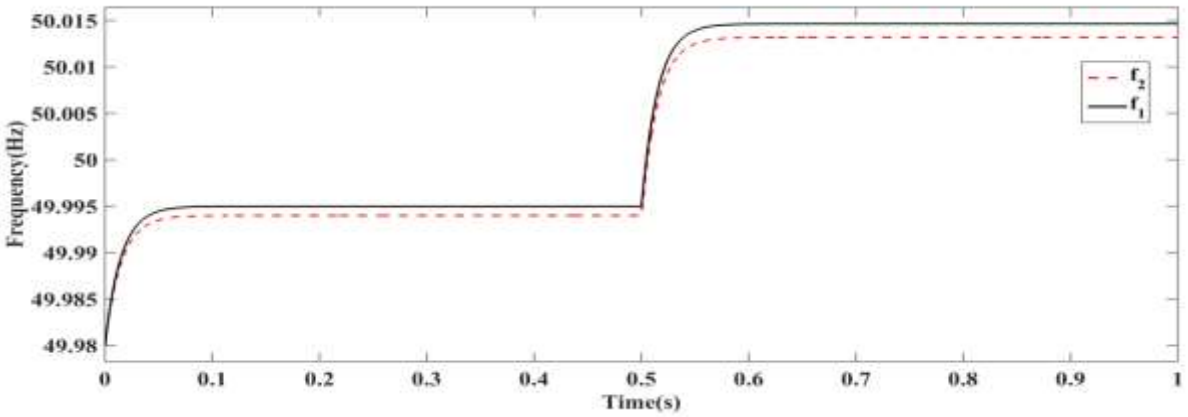

Figure 34: Parallel inverter output frequency using secondary control with virtual inductor under inductive line impedance.

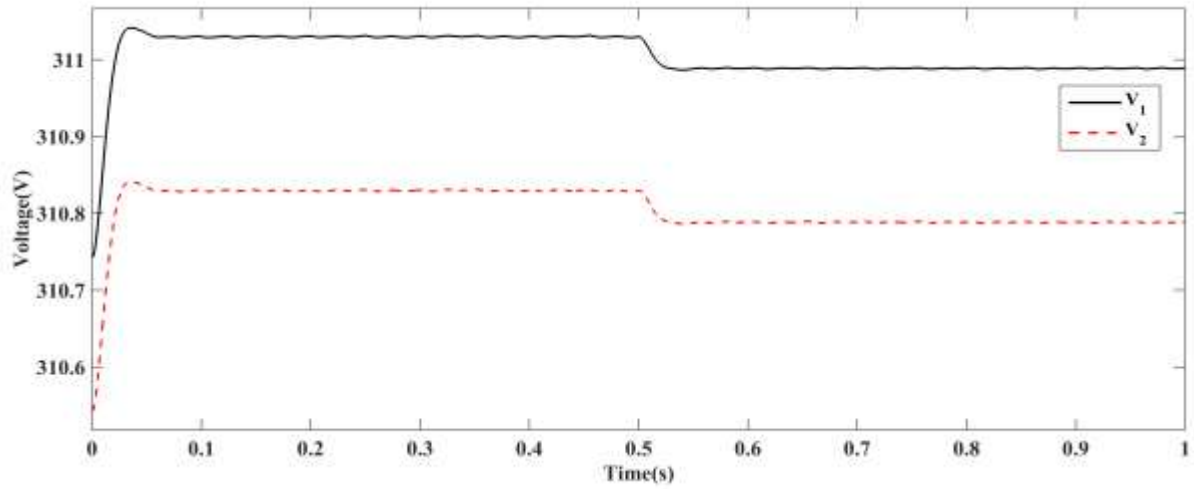

Figure 35: Parallel inverter output voltage using secondary control with virtual inductor under inductive line impedance.

Power sharing of parallel inverters is investigated with common load of P_{load} = 1200 W, Q_{load} = 25 VAR and at 0.5 s sudden local load value of P_{load} = 600 W, Q_{load} = 25 VAR is added to verify the dynamic response and line impedance of $R_{1Line} + jX_{1Line}$ = 0.001+j0.2 Ω, $R_{2Line} + jX_{2Line}$ = 0.002+j0.3 Ω. *P-f/Q-V* droop control based on virtual inductors with secondary control can reduce the influence of line impedance difference on the parallel DG inverters by setting the total output impedance of the DG inverters to be inductive, which improves decoupling of power and improves the proportional load sharing P_1=597 W, P_2=596 W, Q_1=23 VAR, Q_2=22 VAR and at load change at 0.5 s, P_1=894 W, P_2=892 W, Q_1=46 VAR, Q_2=44 VAR as shown in the Fig. 32-33 and frequency variation of DG inverters is within the range of 49.99 Hz to 50.01 Hz, the maximum fluctuation of 0.004 Hz as shown in the Fig. 34. Voltage variation of DG inverters is V_1=311.1 V, V_2=310.9 V as shown in the Fig. 35. Thus, the proposed secondary control for *P-f/Q-V* droop control, ensures voltage amplitude and frequency are restored to the rated value of 50 Hz and 311 V.

Case 5: Power sharing analysis of Secondary control with *P-V/Q-f* droop control under resistive line impedance using different ratings DG inverters.

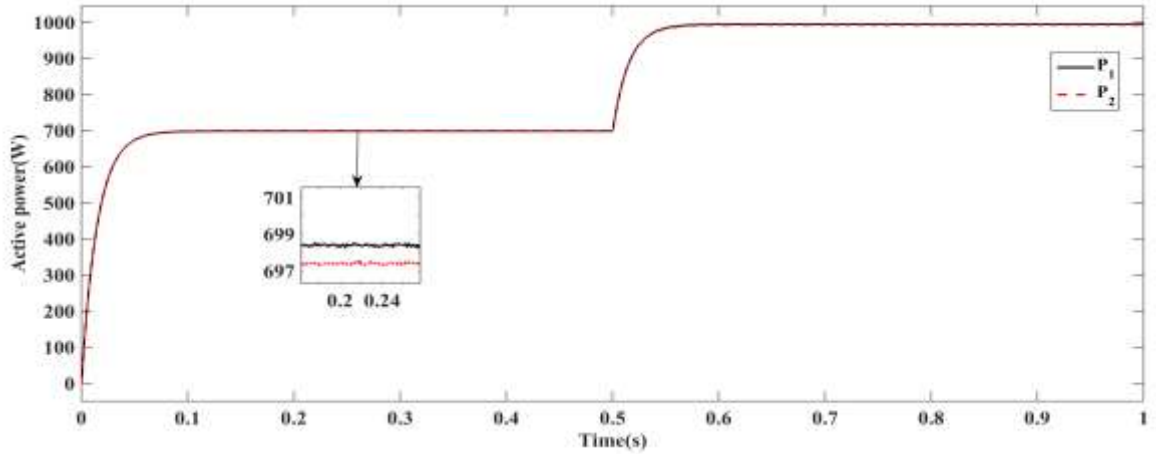

Figure 36: Active power sharing using secondary control with different DG ratings under resistive line impedance.

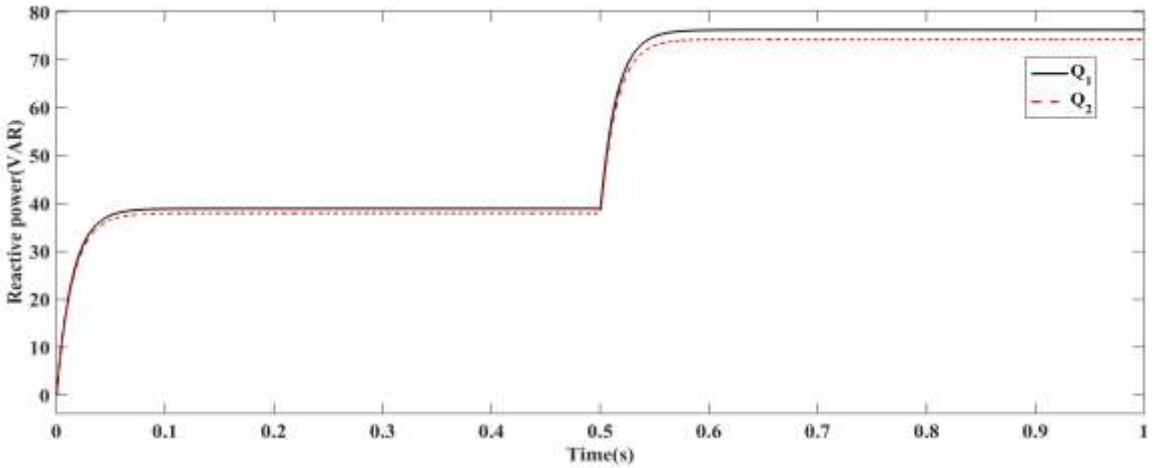

Figure 37: Reactive power sharing using secondary control with different DG ratings under resistive line impedance.

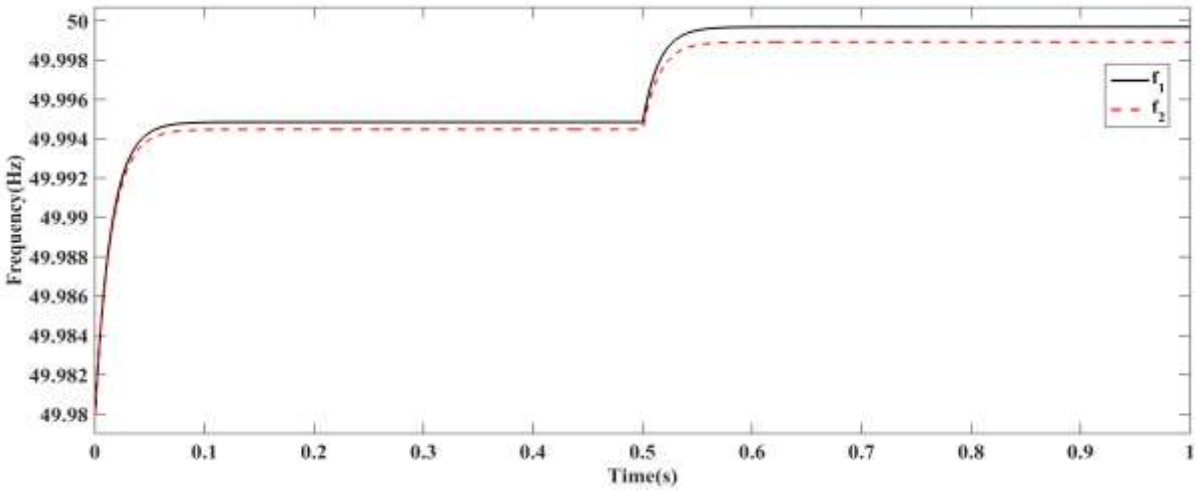

Figure 38: Parallel inverter output frequency using secondary control with different DG ratings under resistive line impedance.

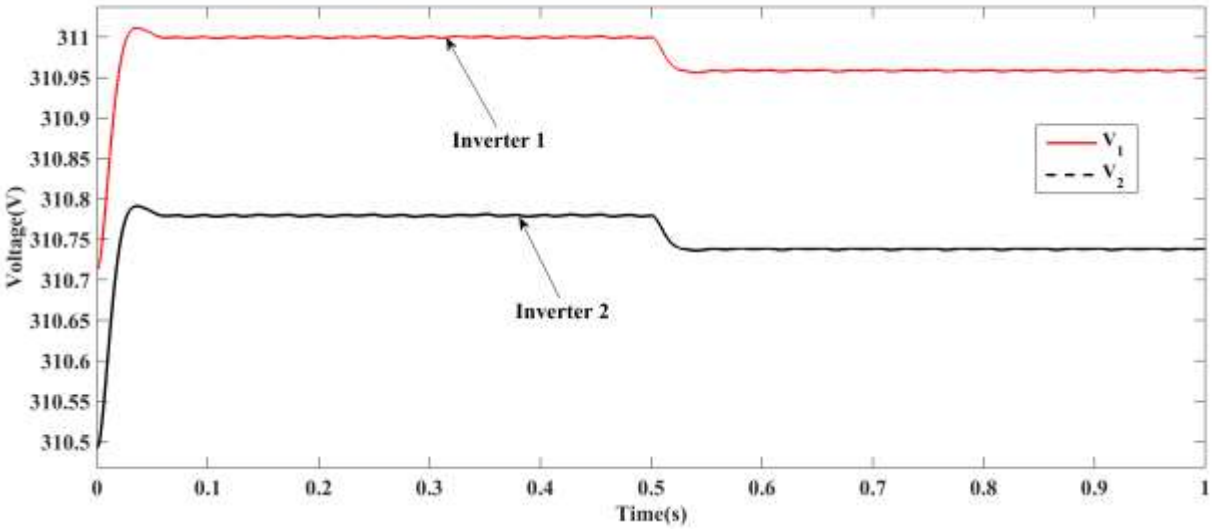

Figure 39: Parallel inverter output voltage using secondary control with different DG ratings under resistive line impedance.

Power sharing of parallel inverters is investigated with common load of P_{load} = 1400 W, Q_{load} = 80 VAR and at 0.5 s sudden local load value of P_{load} = 600 W, Q_{load} = 80 VAR is added to verify the dynamic response and line impedance of $R_{1Line} + jX_{1Line}$ =0.5+j0.001 Ω, $R_{2Line} + jX_{2Line}$ = 0.6+j0.002 Ω. *P-V/Q-f* droop control based on virtual resistors with secondary control can reduce the influence of the line impedance difference on the parallel inverters by setting the total output impedance of the DG inverters to be resistive, which improves decoupling of power and improves the proportional load sharing P_1=697 W, P_2=696 W, Q_1=38 VAR, Q_2=37 VAR and at load change at 0.5 s, P_1=994 W, P_2=992 W, Q_1=76 VAR, Q_2=74 VAR as shown in the Fig. 36-37 and frequency variation of DG inverters is within the range of 49.98 Hz to 50 Hz, the maximum fluctuation of 0.004 Hz as shown in the Fig. 38. Voltage variation of DG inverters is V_1=311 V, V_2=310.75 V as shown in the Fig. 39. Thus, the proposed secondary control for *P-V/Q-f* droop control with different DG ratings under resistive line impedance, ensures voltage amplitude and frequency are restored to the rated value of 50 Hz and 311 V.

Case 6: Power sharing analysis of Secondary control with *P-f/Q-V* droop control under inductive line impedance using different rating DG inverters.

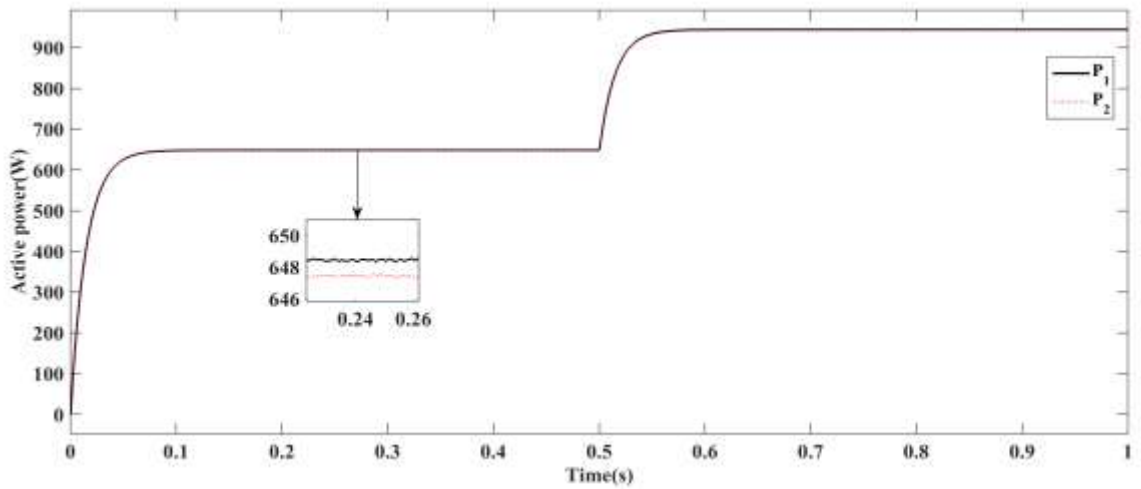

Figure 38: Active power sharing using secondary control with different DG ratings under inductive line impedance.

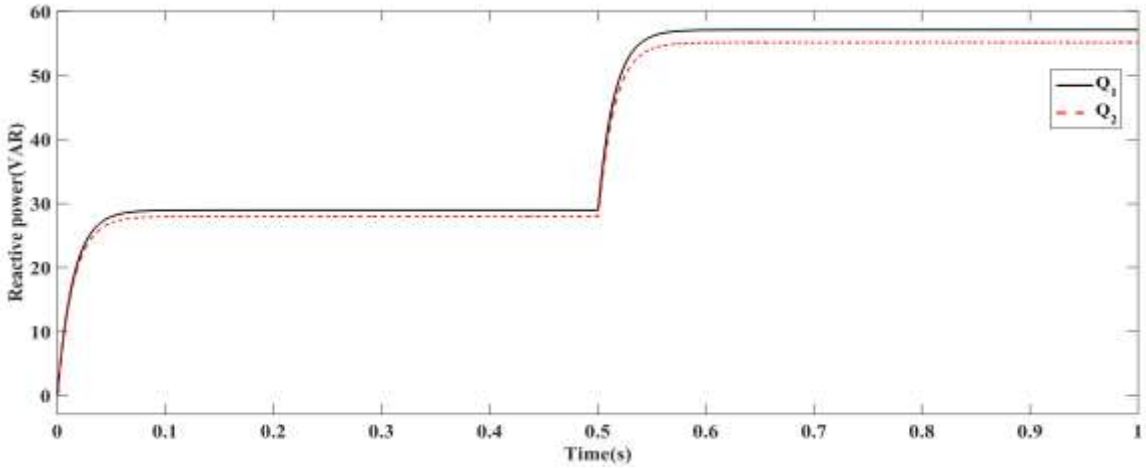

Figure 39: Reactive power sharing using secondary control with different DG ratings under inductive line impedance.

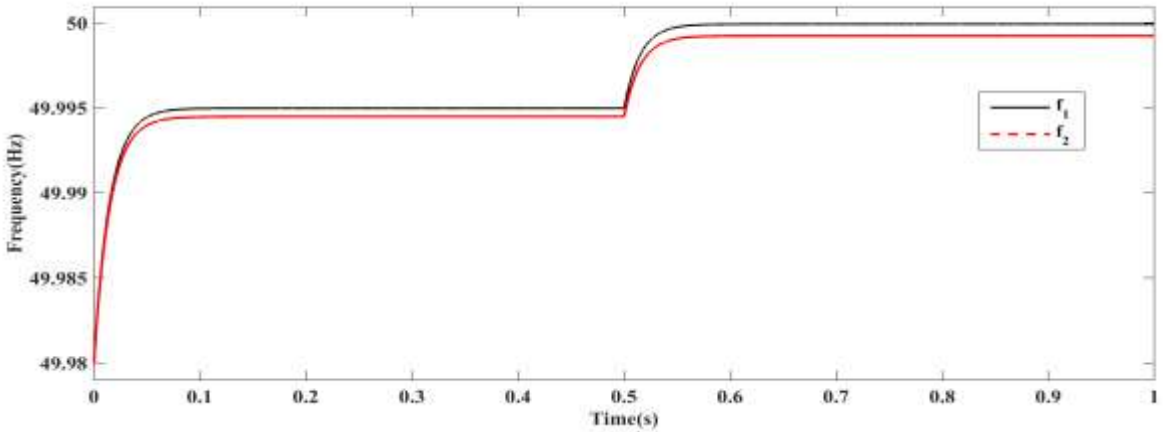

Figure 40: Parallel inverter output frequency using secondary control with different DG ratings under inductive line impedance.

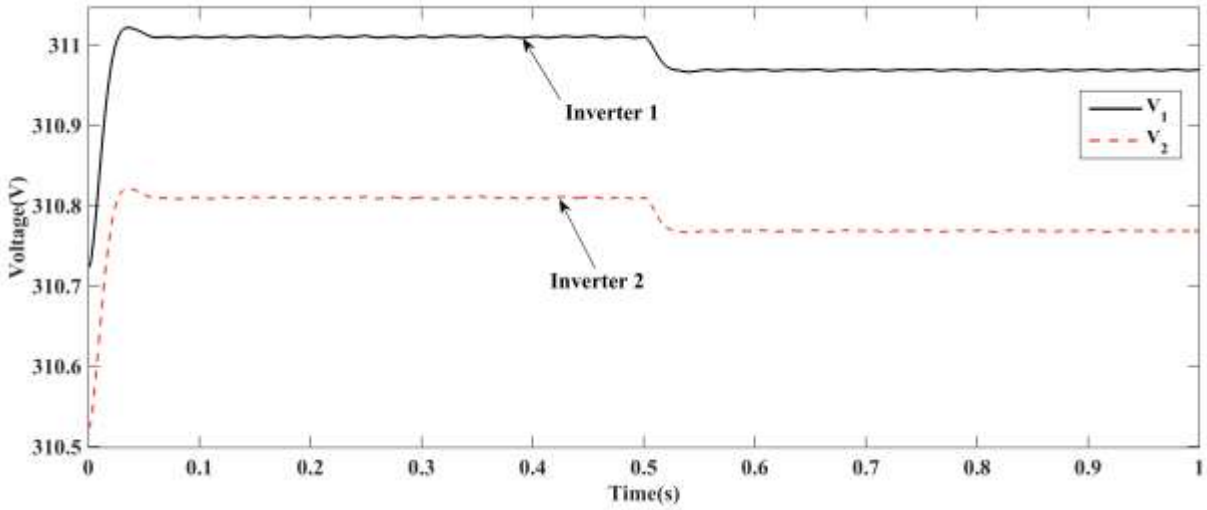

Figure 41: Parallel inverter output voltage using secondary control with different DG ratings under inductive line impedance.

Power sharing of parallel inverters is investigated with common load of P_{load} = 1300 W, Q_{load} = 60VAR and at 0.5 s sudden local load value of P_{load} = 600 W, Q_{load} = 60VAR is added to verify the dynamic response and line impedance of $R_{1Line} + jX_{1Line}$ = 0.001+j0.2 Ω, $R_{2Line} + jX_{2Line}$ = 0.002+j0.3 Ω. *P-f/Q-V* droop control based on virtual inductors with secondary control can reduce the influence of line impedance difference on the parallel DG inverters by setting the total output impedance of the DG inverters to be inductive, which improves decoupling of power and improves the proportional load sharing P_1=647W, P_2=646W, Q_1=28VAR, Q_2=27VAR and at load change at 0.5 s, P_1=944W, P_2=942W, Q_1=56VAR, Q_2=54 VAR as shown in the Fig. 38-39 and frequency variation of DG inverters is within the range of 49.99Hz to 50Hz, the maximum fluctuation of 0.004 Hz as shown in the Fig. 40. Voltage variation of DG inverters is V_1=311.1 V, V_2=310.9 V as shown in the Fig. 41. Thus, the proposed secondary control for *P-f/Q-V* droop control with different DG ratings under resistive line impedance, ensures voltage amplitude and frequency are restored to the rated value of 50Hz and 311V.

Appendix A

Table 1: Parameters of Parallel DG inverters(3KVA Rating)

Symbol	Value	Description
f_s	10 kHz	Inverter switching frequency.
L	4 mH	Filter inductor.
C	10 µF	Filter capacitor.
r	0.1 Ω	Filter inductor equivalent resistance.
V_{dc}	700 V	DC link voltage.
f	50 Hz	Fundamental frequency.
R_v	1 Ω	Virtual resistors.
L_v	5 mH	Virtual inductors.
m_1,m_2 n_1,n_2	0.000025 rad/s/W, 0.0014 V/VAR	*P-f/Q-V* droop coefficients.
n_1,n_2 m_1,m_2	0.0014 V/W, 0.000025 rads/VAR	*P-V/Q-f* droop coefficients.
m_1^*, m_2^*	0.025 rad/s/W,	Improved *P-f/Q-V* droop coefficients.
n_1^*, n_2^*	0.14 V/W,	Improved *P-V/Q-f* droop coefficients.
V_o	311 V	Output voltage of inverter(microgrid system voltage).
K_{ap}, K_{ai}	0.8, 20	PI control parameter for improved *P-f/Q-V* droop control.
K_{bp}, K_{bi}	0.8, 20	PI control parameter for improved *P-V/Q-f* droop control.

Table 2: Electrical parameters of different lines

Type of line	R(Ω/Km)	X(Ω/Km)	R/X
Low voltage line	0.642	0.083	7.70
Medium voltage line	0.161	0.190	0.85
High voltage line	0.06	0.191	0.31

Table 3: Parameters of Parallel DG inverters(3KVA, 9KVA Rating)

Symbol	Value	Description
f_s	10 kHz	Inverter switching frequency.
L	7mH	Filter inductor.
C	20 µF	Filter capacitor.
r	0.2 Ω	Filter inductor equivalent resistance.
V_{dc}	700 V	DC link voltage.
f	50 Hz	Fundamental frequency.
R_v	2 Ω	Virtual resistors.
L_v	6 mH	Virtual inductors.
m_1 m_2 n_1 n_2	0.000025 rad/s/W, 0.0005 rad/s/W, 0.0014V/VAR, 0.002 V/VAR.	*P-f/Q-V* droop coefficients.
n_1, n_2 m_1 m_2	0.0014 V/W, 0.002 V/VAR, 0.000025 rad/s/VAR, 0.0005 rad/s/W.	*P-V/Q-f* droop coefficients.
m_1^*, m_2^*	0.025 rad/s/W,0.05rad/s/W.	Improved *P-f/Q-V* droop coefficients.
n_1^*, n_2^*	0.14 V/W,0.2 V/W	Improved *P-V/Q-f* droop coefficients.
V_o	311 V	Output voltage of inverter(microgrid system voltage).
K_{ap}, K_{ai}	1.2, 25	PI control parameter for improved *P-f/Q-V* droop control.
K_{bp}, K_{bi}	1.4, 28	PI control parameter for improved *P-V/Q-f* droop control.

5. Conclusion

In this paper, analysis of improved *P-f/Q-V* and *P-V/Q-f* droop control with secondary control for DG parallel inverters in microgrid is proposed considering line and output impedance. Proportional integral controller is adopted to ensure accurate tracking of the output voltage of the inverter to the reference value and the influence of the controller parameters on the voltage closed loop transfer function and the equivalent output impedance of the inverter is analyzed. In order to match the total output impedance of the inverter and line impedance in parallel, the *P-V/Q-f* and *P-f/Q-V* droop control strategy based on the inductive and resistive virtual impedance is adopted to improve the total output impedance of the inverter through the virtual impedance. The proposed *P-f/Q-V* and *P-V/Q-f* droop control ,adaptively compensates the virtual resistor and inductor voltage drop to improve output voltage amplitude accuracy to the reference value. Simulation results show the rationality and effectiveness of the proposed improved control method.

6. References

[1] Guerrero J M, Blaabjerg F, Zhelev T, Hrmmer K, Monmasson E, Jemei S, Comech, Frau J I. Distributed generation: towards a new energy paradigm. IEEE Industrial electronics magazine, 2010, 1(4): 944-953.

[2] Chowdhury A A S, Agarwal K, Dono Koval. Reliability modeling of distributed generation in conventional distribution systems planning and analysis. IEEE Transactions on industry applications, 2003, 39(5): 1493-1498.

[3] Furkan A, Mohammad S A. Feasibility study,design and implementation of smart polygeneration microgrid at AMU. International journal of Sustainable cities and society,2017,35:309.322.

[4] Nayanar V, Kumaresan N, Gounden N G A.Wind driven SEIG supplying DC microgrid through a single stage power converter. International journal of engineering Science and technology, 2016,19(3):1600-1607.

[5] Lasseter R H. Microgrids. In: Proceedings of Power Engineering Society Winter meeting, 2002, 305-308.

[6] Chengshan W, Zhangang Y, Shouxiang W, Yanbo C. Analysis of structural characteristics and control approaches of experimental microgrid systems. Automation of Electric Power Systems, 2010, 34(1): 99-105. (in Chinese).

[7] Zhang Li , Wu T, Xing Y, K. Sun, Guerrero J M. Power control of dc microgrid using dc bus signaling. IEEE Twenty-sixth Applied power electronics conference and exposition, 2011, 1-7.

[8] Wu T F, Chen Y K , Huang Y H. 3C strategy for inverters in parallel operation achieving an equal current distribution. IEEE Transactions on Industrial Electronics, 2000, 47(2): 273-281.

[9] Guerrero J M, Hang L, Uceda J. Control of distributed uninterruptible power supply systems. IEEE Transactions on Industrial Electronics, 2008, 55(8): 273-281.

[10] Y Pei, Jiang, X Yang, Z Wang. Auto master slave control technique of parallel inverters in distributed AC power systems and UPS. In: Proceedings of IEEE PESC, 2004, 2050-2053.

[11] Chandorkar M C, Divan D M, Adapa R. Control of parallel connected inverters in standalone ac supply systems. IEEE Transactions on Industry Applications, 1993, 29(1): 136-143.

[12] Guerrero J M, Chandorkar M C, Lee T L, Loh P C. Advanced control architectures for intelligent microgrids-Part-I: Decentralized and Hierarchical control. IEEE Transactions on Industrial Electronics, 2013, 60(4): 1254-1262

[13] Guerrero J M, Vicuna L G de, Matas J, Castilla M, Miret J. A wireless controller to enhance dynamic performance of parallel inverters in distributed generation systems. IEEE Transactions on Power Electronics, 2004, 19(5): 1205-1213.

[14] Vandoorn T L, DeKooning J D M, Meersman B, Guerrero J M, Vandevelde L. Automatic power sharing modification of P/V droop controllers in low voltage resistive microgrids. IEEE Transactions on Power Electronics, 2012, 27(4): 2318-2325.

[15] Yao L, Hua H, Mei S, Yao S, Huibin C, Xi L. A control strategy of reactive power sharing for parallel distributed microsources. Journal of Central South University, 2015, 46(2): 523-533.

[16] Hang H, Liu Y, Sun Y, Su M, Guerrero J M. An improved reactive power sharing in islanded microgrid. IEEE Transactions on Power Electronics, 2015, 30(6): 313-3141.

[17] Qiming C, Siyuan C, Yinman C, Xiaolong Y, Qiang Z. Multiple master slave mixed coordinated control for microgrid based on improved droop control. Automation of electric power systems, 2016, 40(20): 69-74. (in Chinese).

[18] Wu T, Liu Z, Liu S W, You Z. A unified virtual power decoupling method for droop controlled parallel inverters in microgrids. IEEE Transactions on Power Electronics, 2016, 31(8): 5587-5603.

[19] Xiaofeng S, Juan W, Yanjun T, Li Xin. Control of DG connected inverters based on self adaptable adjustment of droop coefficient. Proceedings of the CSEE, 2013, 33(36): 71-78. (in Chinese).

[20] Guerrero J M, Vicuna L G, Mata J. Output impedance design of parallel connected ups inverters with wireless load sharing control. IEEE Transactions on Industrial Electronics, 2005, 52(4): 1126-1135.

[21] Xiongfei Wang, Yun Wei Lei, Frede Blaabjerg, Poh chiang Loh. Virtual impedance based control for voltage source and current source converters. IEEE Transactions on Power Electronics, 2015, 30(12): 7019-7037.

[22] Chengshan W, Zhaoxia X, Shouxiang W. Multiple feedback loop control scheme for inverters of the microsource in microgrids. Transactions of China Electro Technical society, 2009, 24(2): 100-107. (in Chinese).

[23] Brabandere K D, Bolsens B, Van J. A voltage and frequency droop control method for parallel inverters. IEEE Transactions on Power Electronics, 2007, 22(4), 1107-1115.

[24] Mingrui Z, Zhichao Du, Shaobo W. Research on Droop control strategy and parameters selection of microgrids. Transactions of China Electro Technical Society, 2014, 29(2): 136-144. (in Chinese).
[25] Xin C, Changhua Z, Qi H. Small signal stability analysis of microgrid using droop control with differential term. Automation of Electric Power System, 2017, 41(3): 46-53. (in Chinese).
[26] Yajuan G, Guerrero J M, Zhao X, Vasquez J C, Guo X. A new way of controlling parallel connected inverters by using synchronous reference frame virtual impedance loop part-I:control principle. IEEE Transactions on Power Electronics, 2016, 31(6): 4576-4593.
[27] Yajuan G, Weiyang W, Xiaoqiang G. Control strategy for three phase inverters dominated microgrid in autonomous operation. Proceedings of the CSEE, 2011, 31(33): 52-60.
[28] Yan Li, Yun we Li. Virtual frequency voltage frame control of inverter based low voltage microgrid. IEEE Electrical Power and Energy Conference, 2009, 1-6.
[29] Guerrero J M, Berbel N ,devicuna L G, Matas J, Miret J, Castilla M. Droop control method for the parallel operation of online uninterruptible power systems using resistive output impedance. IEEE Twenty first Annual Applied Power Electronics Conference and Exposition, 2006, 1716-1722.
[30] Zhang X , Liu J, Liu T, Zhou L. A novel power distribution strategy for parallel inverters in islanded mode microgrid. Twenty-Fifth Annual Applied Power Electronics Conference and Exposition, 2010, 2116-2120.
[31] Wei Y C, Min Matas J, Guerrero J M, Qian Z M. Design and analysis of the droop control method for parallel inverters considering the impact of the complex impedance on the power sharing. IEEE Transactions on Industrial Electronics, 2011, 58(2): 576-587.
[32] Zmood D N, Holmes D G, Bode G H. Frequency domain analysis of three phase linear current regulators. IEEE Transactions on Industry Applications, 2001, 37(2): 601-610.

[33] Javad F, Henry S, Ben B, Ray O, Karinhinzer J E H. High stability adative microgrid control method using fuzzy logic. International journal of Sustainable cities and society,2016,25:309-322.